Comprehensive analysis of miRNA-mRNA/lncRNA during gonadal development of triploid female rainbow trout (Oncorhynchus mykiss)

Tianqing Huang
Chinese Academy of Fishery Sciences
Wei Gu
Chinese Academy of Fishery Sciences
Enhui Liu
Chinese Academy of Fishery Sciences
Xiulan Shi
Chinese Academy of Fishery Sciences
Bingqian Wang
Chinese Academy of Fishery Sciences
Gefeng Xu (xugefeng@hrfri.ac.cn)
Chinese Academy of Fishery Sciences
Zuochun Yao
Chinese Academy of Fishery Sciences

Research article

Keywords: Triploid, fertility, gonadal development, rainbow trout, long non-coding RNAs (lncRNA), microRNAs (miRNA), competing endogenous RNAs (ceRNA)

Posted Date: December 10th, 2020

DOI: https://doi.org/10.21203/rs.3.rs-31357/v2

Version of Record: A version of this preprint was published at Genomics on November 1st, 2021. See the published version at https://doi.org/10.1016/j.ygeno.2021.08.018.

Abstract

Background: Chromosomal ploidy manipulation is one of the means to create excellent germplasm. Triploid fish could provide an ideal sterile model for the mechanism research of abnormality in meiosis. The complete understanding of the coding and noncoding RNAs regulating sterility caused by meiosis abnormality is still not well understood.

Results: By high-throughput sequencing, we compared the expression profiles of gonadal mRNA, long non-coding RNA (lncRNA), and microRNA (miRNA) at different developmental stages [65 days post fertilisation (dpf), 180 dpf, and 600 dpf] between the diploid (XX) and triploid (XXX) female rainbow trout. A majority of differentially expressed (DE) RNAs were identified, and 22 DE mRNAs related to oocyte meiosis and homologous recombination were characterized. The predicted miRNA-mRNA/lncRNA networks of 3 developmental stages were constructed based on the target pairs of DE lncRNA-miRNA and DE mRNA-miRNA. According to the networks, meiosis-related gene of *ccne1* was targeted by dre-miR-15a-5p_R+1, and 6 targeted DE lncRNAs were identified. Also, RT-qPCR was performed to validate the credibility of the network.

Conclusions: This study explored the potential interplay between coding and noncoding RNAs during the gonadal development of polyploid fish. It provides full insights into polyploidy-associated effects on fertility of fish. These differentially expressed coding and noncoding RNAs provide a novel resource for studying genome diversity of polyploid induction.

Background

The genome duplications in the natural environment provide favorable opportunity for new genes and traits formation of species, which is one of the main driving forces for species evolution (Comai, 2005; Leitch and Leitch, 2008; Van de Peer et al., 2009; 2017). In practice, the artificial induction of polyploidy is of great significance to aquaculture production, which could also provide research models for studying the genome diversity and adaptation (Francesc et al.,2009). The population of triploid fish often shows signs of rapid growth and high resistance (Park et al.,2016; Nwachi et al., 2016; Gregory et al.,2014). More strikingly, most triploid fish has been reported to be sterile because of the imbalance of nuclear-cytoplasmic ratio, the disorders of homologous chromosome pairing during meiosis or the epigenetic instability (Comai, 2005), which would lead to produce abnormal gametes and the cessation of gonad development (Benfey, 1999; Tiwary et al., 2004). The sterility of triploid fish plays important roles in population density control and resource conservation (Taranger et al., 2015; Glover et al., 2018). In addition, triploid fish could provide an ideal sterile model for the mechanism research of abnormality in meiosis. As for triploid male trouts, the testes could normally develop, even if they do not produce fertile spermatozoa (Krisfalusi et al.,1999). The sterile female monosex populations were more popular in production practice. All-female triploid rainbow trout were focused in this study.

Multiple studies have shown that long non-coding RNAs (lncRNA) participate in many reproduction biological processes, such as sexual reproduction (Zhang et al., 2014), gonadal development (Taylor et al., 2015), and gametogenesis (Herrera et al., 2004; Laiho et al., 2013). miRNA could specifically target mRNA of the genes to regulate gene expression, and exerts important regulatory functions in various reproduction events (Chen et al,. 2016; Reza et al., 2019; Shu et al.,2019). The global lncRNAs and repertoire of miRNA in rainbow trout genome had been identified, and tissue-specific lncRNAs had been characterized (Al-Tobasei et al., 2016; Juanchich et al., 2016) The potential coding and noncoding RNA interaction during muscle atrophy between diploid and triploid rainbow trout had been investigated (Paneru et al., 2018). However, a complete understanding of the mechanism regulating sterility caused by meiosis abnormality is still not well understood. So the regulatory mechanism of triploidization on female sterility at the transcriptional or post-transcriptional level should be studied further.

The aim of this study was to better understand the polyploidy-associated effects on development of fish gonad. The differentially expressed (DE) mRNAs, miRNAs, and lncRNAs between diploid (XX) and triploid (XXX) rainbow trout gonads at different developmental stages were identified, the DE mRNAs related to oocyte meiosis and chromosome homologous recombination were characterized. The predicted miRNA-mRNA/lncRNA network regulating gonad development was constructed based on miRNA-mRNA and miRNA-lncRNA pairs, and the lncRNAs which affect indirectly the expressions of meiosis-related mRNAs were screened out. In general, our results provide full insights into polyploidy-associated effects on gonad development, and especially allow for a profound understanding of the differences in the transcriptome between fertile diploid and sterile triploid rainbow trout.

Results

Identification of DE mRNAs, DE lncRNAs, and DE miRNAs during gonadal development

According to a previous study, rainbow trout showed the presence of undifferentiated gonads before 67 dpf, the gonad was composed mainly of primordial germ cells (PGCs) at this period (Feist & Schreck, 1996). The gonadal development of triploid rainbow begins to show abnormal characteristics after 154 dpf, and the gonadal morphology was very different between diploid and triploid after 574 dpf (Xu et al., 2016). The histological analysis of gonadal morphology of 180 dpf and 600 dpf were shown in Fig. S1. The gonads of diploid were consisted mainly of oocyte at different phase, while the somatic cells took up most of the gonads of triploid. For the above reasons, gonadal tissues of 65 dpf, 180 dpf, and 600 dpf were chosen for transcriptome sequencing. The principal component analysis (PCA) plot of our samples was as shown in Supplementary Fig. S2. Transcripts from gonads of the same developmental period but different biological replicates tended to cluster together. As compared to the diploid (XX), the results showed that 425 DE mRNAs at 65 dpf (244 up and 181 down), 1, 022 DE mRNAs at 180 dpf (640 up and 382 down), and 2, 408 DE mRNAs at 600 dpf (1, 862 up and 546 down) were identified in the triploid (XXX) (Fig. 1A–C). The overlapped DE mRNAs between two developmental periods were 124, and among three periods were 3 (Fig. 1J). For lncRNAs, 102 DE lncRNAs at 65 dpf (53 up and 49 down), 226 DE lncRNAs at 180 dpf (129 up and 97 down), and 1, 329 DE lncRNAs at 600 dpf (1, 081 up and 248 down) were identified (Fig. 1D–F). Two DE lncRNAs were overlapped among the three periods and 38 DE lncRNAs were overlapped between two developmental periods (Fig. 1K). For miRNAs, 39 DE miRNAs at 65 dpf (23 up and 16 down), 79 DE miRNAs at 180 dpf (21 up and 58 down), and 42 DE

miRNAs at 600 dpf (28 up and 14 down) were characterized (Fig. 1G–I). The overlapped DE miRNAs between 65 dpf and 180 dpf were 4, and 5 DE miRNAs were overlapped between 180 dpf and 600 dpf (Fig. 1L). The sequences of the overlapped DE miRNAs are shown in Table 1. The full DE reports of ballgown runs for each class of transcripts were provided in the supplementary information (Supplementary Table S1-S9). Both mRNA and lncRNA DEGs were retrieved based on q-value < 0.05, whereas miRNA ones on p-value < 0.05.

Functional analysis of DE mRNAs, DE lncRNAs, and DE miRNAs during gonadal development

GO analysis indicated that the differentially expressed mRNAs at each time point were distributed in biological process (BP), cellular component (CC) and molecular function (MF) classifications (Fig. 2). As for up-regulated DE mRNAs of 65 dpf, the most significant enriched BP terms were transport, regulation of transcription and oxygen transport. Pathway analysis demonstrated that the up-regulated mRNAs of 65 dpf were enriched in PPAR signaling pathway, adipocytokine signaling pathway and Notch signaling pathway (Fig. 3A). The most enriched BP terms of down-regulated DE mRNAs of 65 dpf were lipid transport, one-carbon metabolic process and response to type 1 interferon. KEGG pathway analysis revealed that down-regulated DE mRNAs of 65 dpf were most enriched in NOD-like receptor signaling pathway, influenza A and nitrogen metabolism (Fig. 3B). GO analysis showed that the most enriched BP terms of up-regulated DE mRNAs of 180 dpf were in regulation of transcription, signal transduction and multicellular organism development. As for the down-regulated mRNAs of 180 dpf, the most BP terms were enriched in cell adhesion, cell-matrix adhesion, homophilic cell adhesion via plasma membrane adhesion molecules, response to bacterium. Pathway analysis showed that the up-regulated mRNAs of 180 dpf were most enriched in focal adhesion, vascular smooth muscle contraction and ECM-receptor interaction (Fig. 3C), while the down-regulated mRNAs of 180 dpf were most in calcium signaling pathway, fat digestion and absorption, phenylalanine, tyrosine and tryptophan biosynthesis (Fig. 3D). As for DE mRNAs at 600 dpf, GO analysis demonstrated that up-regulated and down-regulated mRNAs were all most enriched in regulation of transcription-DNA templated, transport and signal transduction of BP terms. KEGG pathway analysis revealed that up-regulated mRNAs were enriched in neuroactive ligand-receptor interaction, cell adhesion molecules (CAMs), calcium signaling pathway, ECM-receptor interaction and Hipoo signalling pathway (Fig. 3E), and down-regulated mRNAs were enriched in lysosome, complement and coagulation cascades, PPAR signaling pathway and Ras signaling pathway (Fig. 3F). GO enrichment analysis showed that the overlapped DE mRNAs were mostly enriched in regulation of transcription, DNA template, protein phosphorylation, regulation of Rho protein signal transduction, cell adhesion and regulation of GTPase activity of BP terms. The most significantly enriched CC terms were cytoplasm, integral component of membrane and membrane. The most significantly enriched MF terms were metal ion binding, zinc ion binding and ATP binding (Fig. 4). The KEGG analysis showed that the most enriched pathways were synaptic vesicle cycle, arginine and proline metabolism and measles (Table 2). The 38 overlapped DE lncRNAs had unknown functions. As for the overlapped DE miRNAs, miR-26a (Kang et al., 2017) and miR-1388 (Yang et al., 2018) have been proven to be correlated with gonadal development in fish.

The DE mRNAs enriched in the pathways of oocyte meiosis and homologous recombination were analysed in different developmental periods of diploid and triploid. Results showed that *sycp3* (synaptonemal complex protein 3) were differentially expressed at 65 dpf, *calml4* (calmodulin-like protein 4), *cpeb2* (cytoplasmic polyadenylation element-binding protein 2), *adcy6* (adenylate cyclase type 6), *dmc1* (meiotic recombination protein DMC1/LIM15 homolog), *kank1* (KN motif and ankyrin repeat domain-containing protein 1), *kank4* (KN motif and ankyrin repeat domain-containing protein 4), *ppp1cb* (Serine/threonine-protein phosphatase PP1-beta catalytic subunit), *pvalb1* (parvalbumin 1) were DE mRNAs at 180 dpf. At 600 dpf, *sycp2* (synaptonemal complex protein 2), *sycp3*, *dmc1*, *adcy6*, *recql4* (ATP-dependent DNA helicase Q4), *plk1* (serine/threonine-protein kinase PLK1), *cpeb4* (cytoplasmic polyadenylation element-binding protein 4), *cdc25c* (M-phase inducer phosphatase 3), *f-box5* (F-box protein 5), *ccnb1* (cyclin-B1), *ccne1* (cyclin-E1), *ccne2* (cyclin-E1), *aurkc* (aurora kinase C), *pttg1* (securin), *mos* (MOS proto-oncogene) in oocyte meiosis or homologous recombination pathway were differentially expressed (Table 3). A network of protein protein interaction (PPI) was constructed according to the functions of DE mRNAs (Fig. 5). In this network, *sycp2*, *sycp3* and *dmc1* played main roles in the assembly of synaptonemal complexes and normal meiotic chromosome synapsis during oocyte development (Kouznetsova et al., 2005; Anjali et al., 2020Chen et al., 2016). *Ccne1*, *ccne1* and *ccnb1* belonged to the cyclin family, and were essential for the control of the cell cycle (Sauer et al., 1995). The other genes, such as *ppp1cb* and *pttg1*, played vital roles in chromosome stability (Barker et al., 1994; Manyes et al., 2018).

Construction of ceRNA network of miRNA-mRNA/lncRNA

Three predicted miRNA-mRNA/lncRNA interaction networks with up- and down-regulated nodes had been established for each developmental stage, which was integrated from the relationship between DE lncRNA-miRNA and DE mRNA-miRNA using perl scripts. The information including all the above interactions was imported into Cytoscape to construct predicted miRNA-mRNA/lncRNA interaction networks. The network of 65 dpf consisted of 10 miRNAs, 13 lncRNAs and 13 mRNAs (Fig. 6A). The network of 180 dpf was composed of 45 miRNAs, 50 lncRNAs and 100 mRNAs (Fig. 6B). The predicted network of 600 dpf was more complex, which consisted of 33 miRNAs, 102 lncRNAs and 135 mRNAs (Fig. 6C). According the functional enrichment analysis of DE mRNAs in each developmental stage, the establishment of miRNA-mRNA/lncRNA interaction networks was helpful to predict the regulatory roles of some non-coding RNAs in fish fertility. The overlapped DE miRNAs of three developmental stages were used to construct a network of miRNA-mRNA/lncRNA, which consisted of 43 DE transcripts (6 miRNAs, 12 lncRNAs, and 25 mRNAs) (Fig. 7).

Ccne 1 screened from DE mRNAs related to oocyte meiosis, was targeted by dre-miR-15a-5p_R+1 of DE miRNAs, and 6 DE lncRNAs were analysed to be targeted by this miRNAs (Table 4). These lncRNAs are regarded as competing endogenous RNAs (ceRNA) to bind miRNA competitively and affect *ccne1* expression, indirectly.

Validation of DE miRNAs, DE lncRNAs, and DE mRNAs by qPCR

To verify the credibility of sequencing, 7 miRNAs, 10 lncRNA, and 10 mRNAs were chosen randomly from the RNA-seq. The expression of different ploidy at different developmental stages of these RNAs was detected by RT-PCR. The results show that the relative expression of 7 miRNAs, 10 lncRNA, and 10 mRNAs in triploid (XXX) was almost consistent with the sequencing results, which was compared to the diploid (XX) (Supplementary Table S10). It was also demonstrated that the lncRNA-miRNA-mRNA network was credible. The expression of *ccne1*, the targeted miRNA dre-miR-15a-5p_R+1, and 6 targeted lncRNAs were detected to verify interactions primarily (Fig. 8). Results showed that the expressions of *ccne1* in triploid were significantly lower than that in diploid at 180 dpf and 600 dpf, while higher at 65 dpf (Fig. 8A). The expression levels of dre-miR-15a-5p_R+1 showed an opposite character (Fig. 8B). In addition, the expressions of MSTRG.74687.3, MSTRG.76205.1 and MSTRG.30919.1 showed a negative correlation with dre-miR-15a-5p_R+1 (Fig. 8C).

Discussion

The fourth round of whole-genome duplication (WGD), which is referring to the salmonid-specific autotetraploidization event (Ss4R), occurred in the common ancestor of salmonids (Allendorf et al., 1984; Near et al., 2012; Jaillon et al., 2004). Salmonids thus appear to provide an unprecedented opportunity for studying evolution and adaption of a duplicated vertebrate genome. In rainbow trout, half of the duplicated protein-coding genes were lost mostly through pseudogenization, while almost all miRNA genes have been retained as duplicated copies (Berthelot et al., 2014). So the post-translational regulation during genome duplication may play vital roles. The artificial induction of polyploidy had been widely applied in aquaculture production, which is not only of great significance to practice value but also provide models for studying genome diversity and adaptation. Compared to diploids, polyploids must overcome genetic instability and meiosis abnormalities after genome duplication (Stenberg & Saura, 2013). For studying meiosis abnormality, triploid fish could provide a sterile model on account of the disorders of homologous chromosome pairing during meiosis (Cimino, 1972). In this study, we selected gonad tissues of female diploid (XX) and triploid (XXX) *Oncorhynchus mykiss* at 65 dpf, 180 dpf, and 600 dpf developmental period. The differentially expressed mRNAs, miRNAs and lncRNAs at these three-time points might be used to examine the effects of genome duplication on gonadal development.

Based on previous studies, genome-wide lncRNAs had been identified and characterized, and testis expressed the highest number of tissue-specific lncRNAs, which provided a resource for our research (Al-Tobasei et al., 2016). The characterization of rainbow trout miRNA transcriptome from a wide variety of tissue had also been carried out to provide a repertoire for reference (Juanchich et al., 2016). The coding and noncoding genes involved in gonadogenesis-associated muscle atrophy had been characterized between the skeletal muscle of gravid females and sterile rainbow trout. A total of 852 mRNAs, 1,160 lncRNAs and 28 microRNAs were differentially expressed between the two groups (Paneru et al., 2018). However, in our study, the more coding and noncoding genes involved in gonad development had been characterized because the effect of polyploidy induction on fish fertility was more complex.

Many studies have shown that triploid animals are almost sterile due to the unequal disjunction of homologous chromosomes during meiosis, which generates aneuploid gametes or reduces gonadal development (Cimino, 1972). In our study, the 22 DE mRNAs enriched in oocyte meiosis and homologous recombination pathways had been screened out. Among these mRNAs, *sycp2* and *sycp3* are key components of lateral elements (LE) of synaptonemal complex (SC) in meiosis, and they are essential for SC assembly and synapsis (Offenberg et al., 1998; Schalk et al., 1999; Yang et al., 2006; Winkel et al., 2009; Kouznetsova et al., 2005). Researches show that the LE could not form properly in *sycp2* knockout mice, so the SC fails to assembly, leading to the sterility (Yang et al.,2006). The knockout of *sycp3* could lead the apoptosis of spermatogenic cells, accompanied by swelled testis in male mice (Yuan et al., 2000). In zebrafish, *sycp2* is essential for homologous recombination and pairing during the initial stages of meiosis (Takemoto et al., 2020). *Dmc1* is related to homologous recombination, which is only expressed in meiosis (Anjali et al., 2020；Chen et al., 2016). Females and males in the homozygous knockout of *dmc1* are all sterile, gametogenesis is impeded to stagnate in prophase of the first meiotic division (Pittman et al.,1998). In ploypoid cyprinid fish, *dmc1* is directly related to gonad development. *Ccne1* belongs to the gene family of cyclin, and is proved to affect homologous pairing and DNA repair during the first meiotic division, especially to regulate the function of ends of chromosomes (Bonache et al., 2014; Laetitia et al., 2014). In this study, the expression of *ccne1* was proved to be significantly lower in triploid at both 180 dpf and 600 dpf. The dre-miR-15a-5p_R+1 of DE miRNAs was screen out to target with *ccne1*, and its levels in triploid were significantly higher at 180 dpf and 600 dpf, which indicated the expression of *ccne1* may be suppressed by dre-miR-15a-5p_R+1. According to previous research, miR-15a could regulate gametogenesis and gonad development by directly targeting cyclin T2 (*ccnt2*) (Teng et al., 2011). In our study, MSTRG.74687.3, MSTRG.76205.1 and MSTRG.30919.1 of DE lncRNAs were targeted by dre-miR-15a-5p_R+1, and their expressions were negatively correlated with dre-miR-15a-5p_R+1. So these lncRNAs may interact indirectly with the expression of *ccne1*, which could play important roles in meiosis and gonad development.

Among the enriched pathways of DE mRNAs, the Hippo pathway plays an important role in regulating follicle development (Kawashima & Kawamura, 2017). Peroxisome proliferator-activated receptors (PPARs) are important in the reproductive system and are expressed at different levels in the hypothalamic-pituitary-gonadal (HPG) axis (Bogacka et al., 2015). Some studies have demonstrated that PPARs can regulate ovum proliferation, tissue remodelling, and hormone synthesis (Barak et al., 2002). The WNT/CTNNB1 signalling pathway involves many important biological processes, including sex determination, and reproductive system specialisation (Chassot et al., 2008; Mark et al., 2008). These pathways could be speculated to be associated with the gonadal development of rainbow trout.

There are still many unknown functions of lncRNAs and miRNAs in regulating gonadal development. According to ceRNA regulatory mechanisms, gene-encoding mRNA transcripts contain many microRNA response elements (MREs). miRNAs can bind to the mRNAs through MREs to cause mRNA degradation or inhibit its translation (Ye et al., 2008). When lncRNA and mRNA contain the same MREs, they compete for the same type of miRNAs. Hence, lncRNAs indirectly regulate the expression of mRNAs through MREs, thereby regulating their biological functions (Guo et al., 2014). This study constructed effector networks of the three RNA species based on the above reasons for a more in-depth understanding of the effects of ploidy on meiosis and gonadal development.

Many of the maternal RNAs were stored for post-oocyte growth through early embryonic development in the oocytes. The transcripts that overlapped in the Venn diagrams for the three stages may be in part maternal transcripts destine for storage until spawning. Their functions may require a bit deeper delve. The overlapped DE miRNAs in the predicted miRNA-mRNA/lncRNA interaction network constructed in this study indicated that these miRNAs play a role in the normal development of gonads. Among the identified miRNAs, many are worthy of further studies. According to previous studies, miR-26a can regulate gonadal development in *Paralichthys olivaceus* through its target, the *emx2* gene (Yin et al., 2015). miR-26a-5p overexpression can inhibit *TNRC6A* expression and promote the proliferation of the theca cells (Kang et al., 2017). miR-1388 plays an indispensable role in regulating gonadal development in *P. olivaceus* through its target, the *nectin21* gene (Yang et al., 2018). The role of these lncRNAs, mRNAs, and miRNAs from this predicted ceRNA network in gonadal development and meiosis may provide a resource for mechanism research.

Conclusions

In summary, our study was the first to construct the predicted miRNA-mRNA/lncRNA interaction networks that were associated with gonadal development in polyploid fishes. We identified lots of DE mRNAs, DE lncRNAs, and DE miRNAs through screening of different developmental stages and constructed ceRNA effector networks based on the effector relationships of mRNA-miRNA and lncRNA-miRNA. The up-regulated and down-regulated DE mRNAs at different developmental stages were annotated and analysed. At the same time, DE mRNAs related to oocyte meiosis and homologous recombination were characterized. The lncRNAs associated with meiosis in fishes were discovered and identified. This study explored the potential interplay between coding and noncoding RNAs during the gonadal development of polyploid fish. It provides full insights into polyploidy-associated effects on fertility of fish. These differentially expressed coding and noncoding RNAs provide a novel resource for studying genome diversity of polyploid induction.

Methods

Ethics statement

All experiments were performed according to the European Communities Council Directive (86/609/EEC) norms and approved by the Animal Husbandry Department of Heilongjiang Animal Care and Use Committee. All fishes involved in this research were bred following the guidelines of the Animal Husbandry Department of Heilongjiang, P.R. China. All efforts were made to minimise the pain.

Gonadal sampling of rainbow trout

Triploid all-female (XXX) and diploid all-female (XX) rainbow trouts were obtained from Bohai experimental station of Heilongjiang River Fisheries Research Institute (Harbin, China). First of all, diploid all-female trouts (XX) were produced by the blockage of the first cell mitosis (under hydrostatic pressure) of eggs which were fertilised with semen (XY) dealt with ultraviolet. Then the diploid all-females (XX) were fed with the aromatase inhibitor to get pseudo-males (XX) which could produce functional semen. Finally, the triploid all-female eggs were obtained from the normal female eggs (XX) fertilised with pseudo-male semen (XX), and then the fertilised eggs were shocked by hydrostatic pressure to inhibit extrusion of the second polar. The ploidy of eggs was verified by Ploidy Analyser (Sysmex, Japan), the result of ploidy identification of gonad samples were as shown in Supplementary Fig. S3, and the triploid rate could reach up to 99%. The embryos were incubated at 12 °C from fertilisation until 24 days post-fertilisation (dpf) and transferred to a hatch pool at 12+0.2 °C. The fries after hatching at 58 dpf were transferred to a cement pool when they were grown to achieve around 40 g in weight. This study was performed at 12+0.2 °C all the time. To minimize suffering of the fish, before tissue collection, fish were euthanized with an overdose of anaesthesia in MS-222 (Sigma, St. Louis, MO, USA) as reported previously (Chang et al., 2017). The gonadal part of the fry at 65 dpf was isolated under an anatomic microscope. The 3 RNA samples of each ploidy were prepared at each developmental stage, and each of the RNA samples was composed of gonadal tissues from 10 female individuals at 65 dpf, 5 female individuals at 180 dpf and 1 female individual at 600 dpf. All gonads were sampled and stored at – 80 °C for further experiments.

Sequencing and differential expression analysis of mRNAs and lncRNAs

The Trizol reagent (Invitrogen, CA, USA) was used to extract the total RNA, and only RNA integrity number (RIN) >7.0, the RNA samples would be kept for the next experiments. The Epicentre Ribo-Zero Gold Kit (Illumina, San Diego, USA) was used to deplete ribosomal RNA of the total RNA. Under high temperature, RNA fractions were fragmented into small pieces. The mRNA-Seq sample preparation kit (Illumina, San Diego, USA) was used for RNA fragments to reverse-transcription to construct the final cDNA library. The average size for the paired-end libraries was 300 bp (±), and then the paired-end sequencing was performed on an Illumina Hiseq 4000 following the vendor's recommended protocol. Firstly, transcripts that overlapped with the known mRNAs and transcripts shorter than 200 bp were discarded. Cutadapt was used to fastq quality control as following steps: (1) reads with Adaptor were removed; (2) reads containing N (N indicates that the base information cannot be determined) at a rate greater than 5% were removed; (3) low quality (the number of bases with quality value Q≤10 accounts for more than 20% of the whole read) reads were removed. The clean and filtered reads were aligned to the reference genome of *Oncorhynchus mykiss* (https://www.ncbi.nlm.nih.gov/genome/?term=Oncorhynchus%20mykiss, Omyk_1.0) using HISAT (v2.0.4) (min_intron_length=20 max_intron_length=500000). The valid reads and the percentage of mapped reads for each sample were shown as in Supplementary Table. S11. Thereafter, we utilised CPC (Kong et al., 2007) and CNCI (Sun et al., 2013) to predict transcripts having coding potentials. All transcripts with a CPC score of <−1 and CNCI score of <0 were removed. The remaining transcripts were considered as lncRNAs. StringTie (Frazee et al., 2015) was used to estimate the expression level of mRNAs and lncRNAs by calculating FPKM (Punta et al., 2012), the parameter of StringTie was set as stringtie_abundance=1. The differentially expressed mRNAs and lncRNAs were selected with log2 (fold change) >1 or log2 (fold change) <−1 and FDR< 0.05 as significant cutoff values using R package Ballgown (Agarwal et al., 2015), the parameter was set as remove_low_copy=0. The RNA-Seq raw data were

deposited into the repository of SRA-NCBI, the BioProject number of miRNA-suquencing was PRJNA606210, and the number of mRNA and lncRNA sequencing was PRJNA671795.

Sequencing and differential expression analysis of miRNAs

The TruSeq Small RNA Sample Prep Kits (Illumina, San Diego, USA) was used to construct the cDNA libraries. The cDNA product was purified by gel electrophoresis. After recovery, the purified library was concentrated by ethanol precipitation. The cDNA library was validated by DNA-1000 chip (Agilent Technologies 2100 Bioanalyzer, Agilent, CA, USA). The sequencing of cDNA libraries was performed using Illumina Hiseq 2500 through single-read strategy (1 × 50 bp). Raw reads were subjected to the ACGT101-miR tool (LC Sciences, Houston, Texas, USA) to remove adapter dimers, junk, low complexity, common RNA families (rRNA, tRNA, snRNA, snoRNA) and repeats (Ambady et al., 2012). Two aligners (Bowtie and Megablast) were used by ACGT101-miR, and their corresponding parameters were set as the following: Bowtie was used for reads to align against the mRNA sequence of *Oncorhynchus mykiss* (ftp://ftp.ncbi.nlm.nih.gov/genomes/all/GCF/002/163/495/GCF_002163495.1_Omyk_1.0/GCF_002163495.1_Omyk_1.0_cds_from_genomic.fna.gz), Rfam, Repbase and miRBase 22.0 database setting seed length = 16 and mismatch = 1. Megablast was used to align pre-miRNAs against the reference genome applying a 90% identity threshold. The unique sequences mapping to miRNAs' annotated loci on the genome of *O. mykiss* were identified as known miRNAs. The unique sequences mapping to the other arm of *O. mykiss* known pre-miRNAs, opposite to the annotated mature miRNA-containing arm, were considered to be novel 5p- or 3p- derived miRNA candidates. The remaining sequences were mapped to other selected species precursors (with the exclusion of the genome of *O. mykiss*) in miRBase 22.0, and the mapped pre-miRNAs were further aligned against the genome of *O. mykiss* to determine their genomic locations. The above two we defined as known miRNAs. The unmapped sequences were aligned against the genome of *O. mykiss*, and the hairpin RNA structure-containing sequences were predicted from the flank 80 nt sequences using RNAfold software (http://rna.tbi.univie.ac. at/cgi-bin/RNAfold.cgi). The criteria for secondary structure prediction were: (1) number of nucleotides in one bulge in stem (≤12) (2) number of base pairs in the stem region of the predicted hairpin (≥16) (3) cutoff of free energy (kCal/mol ≤-15) (4) length of hairpin (up and down stems + terminal loop ≥50) (5) length of hairpin loop (≤20). (6) number of nucleotides in one bulge in mature region (≤8) (7) number of biased errors in one bulge in mature region (≤4) (8) number of biased bulges in mature region (≤2) (9) number of errors in mature region (≤7) (10) number of base pairs in the mature region of the predicted hairpin (≥12) (11) percent of mature in stem (≥80). Finally, the effective sequences of miRNAs were further analyzed. One-way ANOVA was used to assess the differences between the different groups. The differential expression of the miRNAs based on normalised read counts were assessed through Student's t-test, setting a significance threshold of 0.05 in each performed test.

Construction of ceRNA network of miRNA-mRNA/lncRNA

The DE lncRNAs and 3' UTR sequences of DE mRNAs were predicted as candidate miRNA targets using TargetScan (Agarwal et al., 2015) and miRanda (Betel et al., 2010). The threshold value of TargetScan for seed length scanned against the lncRNAs and 3’ UTRs of mRNAs database was context score percentile > 50, and the threshold free energy (kcal/mol) of miRanda was established as Max_Energy<-10. The miRNA-target selection was performed according to the intersection between the two tools. The output of the ad-hoc perl scripts of DE miRNA-mRNA and miRNA-lncRNA of different developmental period were as shown in Supplementary Table. S12 and Table. S13. The ceRNA regulatory cascades (miRNA-mRNA /lncRNA) were built by local perl scripts. The information including all of the above interaction was imported into Cytoscape (3.7.1) to construct a predicted miRNA-mRNA/lncRNA interaction network.

Functional analysis of DE mRNA

Gene Ontology (GO) enrichment analysis and Kyoto Encyclopaedia of Genes and Genomes (KEGG) pathway analyses were performed on the predicted target DE mRNAs of DE miRNA and DE lncRNAs in the ceRNA network, and DE mRNAs of different developmental period. For the non-model species, the specific steps of functional analysis were as follows: Firstly, the transcripts of the reference *Oncorhynchus mykiss* genome were used to align against the GO (go_20160702) and KEGG (release_78.1) database by Diamond with the parameter of E-value=1*E-5 (Buchfink et al., 2014). The comparison results of all transcripts for each gene which were integrated and removed duplicate were as the functional annotations of GO and KEGG. The local scripts were used for enrichment analysis. Then, the number of significantly DE genes (S gene number), the number of background genes (B gene number), the number of total significantly DE genes (TS gene number) and the number of total background genes (TB gene number) for each GO term/KEGG pathway were counted by GO and KEGG functional annotations. Pval was obtained by hypergeometric test. Both GO terms and KEGG pathways were considered to be significantly enriched with FDR < 0.05.

Validation of RNAs in the network by real-time PCR

Real-time PCR was performed for validation of the RNAs involved in the RNA-Seq. The same RNA samples were used for deep sequencing. The qRT-PCR primers are shown in the Supplementary Table S14. For lncRNAs and mRNAs, the PrimeScript RT Reagent Kit (Takara, Dalian, China) was used for reverse transcription. Real-time PCR was performed using FastStart Universal SYBR® Green Master Mix (Roche, Switzerland) using CFX96 C1000 touch Thermal Cycler (BIO-RAD, America). As for miRNAs, All-in-One™ miRNA qRT-PCR Detection Kit (GeneCopoeia, America) was used for RNA reverse transcription and real-time PCR. According to the analysis of geNorm, the mean values of expression stablility of *GAPDH* and *18s* rRNA at the three detected developmental period were less than 1.5. So the expression was normalised by the expression of *GAPDH* and *18s* rRNA. All experiments were strictly performed following the instructions. The Ct values were measured, and the value of target sequence normalised to reference sequence was calculated as $2^{-\Delta\Delta Ct}$. Data were analysed by one-way ANOVA to denote statistical differences among groups, which were followed by t-Student test was used to determine statistical differences between different groups. Statistical analyses were conducted using SPSS 13.0 software. All data are presented as mean ± standard error of the mean (SEM). Minimum level of significance was fixed in 0.05.

Abbreviations

DEGs: Differentially expressed genes; cDNA: Complementary; RNA: Ribonucleic acid; mRNA: Messenger RNA; miRNA: microRNAs; lncRNA: long non-coding RNA; RNA-Seq: RNA-sequencing; FDR: False discovery rate; dpf: days post fertilization; RIN: RNA integrity number; ceRNA: competing endogenous RNAs.

Declarations

Ethics approval and consent to participate

All experiments were performed according to the European Communities Council Directive (86/609/EEC) norms and approved by the Animal Husbandry Department of Heilongjiang Animal Care and Use Committee.

Consent for publication

Not applicable.

Availability of data and materials

Specific data and local scripts used herein and the gtf and fasta files from the newly identified MSTRG lncRNAs and miRNAs can be provided upon readers request. The cytoscape files for networks could be provided upon request.

Competing interests

The authors declare that they have no competing interests.

Funding

This study was supported by grants from the National Key R&D Program of China (2018YFD0900200), the China Agriculture Research System (CARS-46) and Central Public-interest Scientific Institution Basal Research Fund□CAFS(NO. 2020TD32). The funding agency played no part in study design, data collection and analysis, decision to publish, or preparation of the manuscript.

Author's contributions

T. H. designed and performed the experiments; G. X. analysed the data and checked the manuscript; W. G. and Z. Y. cultured and sampled the fish; E. L. drafted the article; Xiulan Shi submitted and revised the manuscript. T. H. and B. W. reviewed the manuscript. All authors contributed to the manuscript at various stages. All authors have read and approved the manuscript.

Acknowledgements

We thank all individuals who participated in this study.

References

Agarwal, V., Bell, G. W., Nam, J. W., & Bartel, D. P. Predicting effective microRNA target sites in mammalian mRNAs. Elife. 2015;4:e05005. https://doi.org/10.7554/ eLife.05005.001.

Allendorf, F. W. & Thorgaard, G. H. Tetraploidy and the evolution of salmonid fishes. Plenum Press.1984;1-53. https://doi.org/10.1007/978-1-4684-4652-4_1.

Al-Tobasei R, Paneru B, Salem M. Genome-Wide Discovery of Long Non-Coding RNAs in Rainbow Trout. PLoS One. 2016;11(2):e0148940. https://doi.org/10.1371/journal.pone.0148940.

Ambady, S., Wu, Z., & Dominko, T. Identification of novel microRNAs in Xenopus laevis metaphase II arrested eggs. Genesis. 2012;50(3):286-299. https://doi.org/ 10.1002/dvg.22010.

Anjali Gupta Hinch, Philipp W. Becker, Tao Li, et al. The Configuration of RPA, RAD51, and DMC1 Binding in Meiosis Reveals the Nature of Critical Recombination Intermediates. Molecular Cell. 2020;79(4):689-701.e10. https://doi.org/10.1016/j. molcel.2020.06.015

Barak Y, Liao D, He W, et al. Effects of peroxisome proliferator-activated receptor delta on placentation, adiposity, and colorectal cancer. Proceedings of the National Academy of Sciences. 2002;99(1):303-308. https://doi.org/10.1073/pnas. 012610299.

Barker HM, Brewis ND, Street AJ, Spurr NK, Cohen PT. Three genes for protein phosphatase 1 map to different human chromosomes: sequence, expression and gene localisation of protein serine/threonine phosphatase 1 beta (PPP1CB). Biochim Biophys Acta. 1994;1220(2):212. https://doi.org/10.1016/0167-4889(94)90138-4.

Benfey, T., J. The physiology and behavior of triploid fishes. Reviews in Fisheries Science. 1999;7:45–48. https://doi.org/10.1080/10641269991319162.

Berthelot C , Brunet, Frédéric, Chalopin D , et al. The rainbow trout genome provides novel insights into evolution after whole-genome duplication in vertebrates. Nat Commun. 2014;5:3567. https://doi.org/10.1038/ncomms4657.

Betel D, Koppal A, Agius P, et al. Comprehensive modeling of microRNA targets predicts functional non-conserved and non-canonical sites. Genome Biology, 2010;11(8): R90. https://doi.org/10.1186/gb-2010-11-8-r90.

Bogacka I, Kurzynska A, Bogacki M, & Chojnowska K. Peroxisome proliferator-activated receptors in the regulation of female reproductive functions. Folia Histochemica Cytobiologica. 2015;53(3):189-200. https://doi.org/10.5603/fhc.a 2015.0023.

Bonache S, Algaba F, Franco E, et al. Altered gene expression signature of early stages of the germ line supports the pre-meiotic origin of human spermatogenic failure. Andrology. 2014;2(4):596-606. https://doi.org/10.1111/j.2047-2927.2014. 00217.x.

Buchfink, B., Xie, C., & Huson, H. D. Fast and sensitive protein alignment using DIAMOND. Nature Methods. 2014;12(1):59-60. https://doi.org/10.1038/nmeth.3176.

Chang J, Niu H X, Jia Y D, et al. Effects of dietary lipid levels on growth, feed utilization, digestive tract enzyme activity and lipid deposition of juvenile Manchurian trout, Brachymystax lenok (Pallas). Aquaculture Nutrition, 2017;24(2). https://10.1111/anu.12598.

Chassot, A. A., Gregoire, E. P., Lavery, R., Taketo, M. M., de Rooij, D. G., Adams, I. R., & Chaboissier, M. C. RSPO1/beta-catenin signaling pathway regulates oogonia differentiation and entry into meiosis in the mouse fetal ovary. PLoS One. 2011;6(10): e25641. https://doi.org/10.1371/journal.pone.0025641.

Chassot, A. A., Ranc, F., Gregoire, E. P., Roepers-Gajadien, H. L., Taketo, M. M., Camerino, G., de Rooij, D. G., Schedl, A. & Chaboissier, M. C. Activation of beta-catenin signaling by Rspo1 controls differentiation of the mammalian ovary. Hum Mol Genet. 2008;17(9):1264-1277. https://doi.org/10.1093/hmg/ddn016.

Chen J, Cui X, Jia S, et al. Disruption of dmc1 Produces Abnormal Sperm in Medaka (*Oryzias latipes*). Scientific Reports. 2016;6:30912. https://doi.org/10.1038/ srep30912.

Chen L, Zhang BY, Feng GD, Xiang W, Ma YX, Chen H, Chu MX, Wang PQ. The mechanism of miRNA-mediated PGR signaling pathway in regulating female reproduction. Hereditas. 2016;38(1):40-51. https://doi.org/10.16288/j.yczz.15-293.

Cimino MC. Meiosis in triploid all-female fish (Poeciliopsis, Poeciliidae). Science. 1972;175(4029):1484-6. https://doi.org/10.1126/science.175.4029.1484.

Comai L. The advantages and disadvantages of being polyploid. Nat Rev Genet. 2005;6(11):836-846. https://doi.org/10.1038/nrg1711.

Feist, G. & Schreck, C. B. Brain-pituitary-gonadal axis during early development and sexual differentiation in the rainbow trout, Oncorhynchus mykiss. Gen Comp Endocrinol, 1996;102(3):394-409. https://doi.org/10.1006/gcen.1996.0083.

Francesc Piferrer, Andy Beaumont, Jean-Claude Falguière, et al. Polyploid fish and shellfish: Production, biology and applications to aquaculture for performance improvement and genetic containment. Aquaculture. 2009;293(3):125-156. https://doi.org/10. 1016/j.aquaculture.2009.04.036.

Frazee, A. C., Pertea, G., Jaffe, A. E., Langmead, B., Salzberg, S. L. & Leek, J. T. Ballgown bridges the gap between transcriptome assembly and expression analysis. Nat Biotechnol. 2015;33(3):243-246. https://doi.org/10.1038/nbt.3172.

Glover K. A. et al. Three Decades of Farmed Escapees in the Wild: A Spatio-Temporal Analysis of Atlantic Salmon Population Genetic Structure throughout Norway. PloS one. 2018;e43129. https://doi.org/10.1371/journal.pone. 0043129.

Gregory M. Weber, Mark A. Hostuttler, Beth M. Cleveland, et al. Growth performance comparison of intercross-triploid, induced triploid, and diploid rainbow trout. Aquaculture. 2014;433:85-93. https://doi.org/10.1016/j.aquaculture.2014.06. 003.

Guo, L., Zhao, Y., Yang, S., Zhang, H., & Chen, F. An integrated analysis of miRNA, lncRNA, and mRNA expression profiles. Biomed Res Int. 2014;345605. https://doi.org/10.1155/2014/345605.

Guo, X., et al. All-triploid Pacific oysters (Crassostrea gigas Thunberg) produced by mating tetraploids and diploids. Aquaculture. 1996;142:149-161. https://doi.org/ 10.1016/0044-8486(95)01243-5.

Herrera, L., Ottolenghi, C., Garcia-Ortiz, J. E., Pellegrini, M., Manini, F., Ko, M. S., Nagaraja, R., Forabosco, A., & Schlessinger, D. Mouse ovary developmental RNA and protein markers from gene expression profiling. Dev Biol. 2005;279(2): 271-290. https://doi.org/10.1016/j.ydbio.2004.11.029.

Jaillon, O. et al. Genome duplication in the teleost fish Tetraodon nigroviridis reveals the early vertebrate proto-karyotype. Nature. 2004;431(7011):946-57. https://doi.org/ 10.1038/nature03025.

Jaillon, O., et al. Genome duplication in the teleost fish Tetraodon nigroviridis reveals the early vertebrate proto-karyotype. Nature. 2004;431:946-957. https://doi.org/ 10.1038/nature03025.

Juanchich A, Bardou P, Rué O, Gabillard JC, Gaspin C, Bobe J, Guiguen Y. Characterization of an extensive rainbow trout miRNA transcriptome by next generation sequencing. BMC Genomics. 2016;17:164. https://doi.org/ 10.1186/s12864-016-2505-9.

Kang, L., Yang, C., Wu, H., Chen, Q., Huang, L., Li, X., Tang, H., & Jiang, Y. miR-26a-5p regulates TNRC6A Expression and Facilitates Theca Cell Proliferation in Chicken Ovarian Follicles. DNA Cell Biol. 2017;36(11):922-929. https://doi.org/ 10.1089/dna.2017.3863.

Kawashima, I., & Kawamura, K. Regulation of follicle growth through hormonal factors and mechanical cues mediated by Hippo signaling pathway. Syst Biol Reprod Med. 2017;64(1):3-11. https://doi.org/10.1080/19396368.2017.1411990.

Kong, L., Zhang, Y., Ye, Z. Q., Liu, X. Q., Zhao, S. Q., Wei, L., & Gao, G. CPC: assess the protein-coding potential of transcripts using sequence features and support vector machine. Nucleic Acids Res. 2007;35(Web Server issue):W345-349. https://doi.org/10.1093/nar/gkm391.

Kouznetsova, A. SYCP2 and SYCP3 are required for cohesin core integrity at diplotene but not for centromere cohesion at the first meiotic division. Journal of Cell ence. 2005;118(10):2271-8. https://doi.org/10.1242/jcs.02362.

Krisfalusi M, Cloud JG. Gonadal sex reversal in triploid rainbow trout (*Oncorhynchus mykiss*). J Exp Zool. 1999;284(4):466-72. https://doi.org/10.1002/(sici)1097-010x (19990901)284:4<466::aid-jez13>3.3.co;2-7.

Laetitia Martinerie, Marcia Manterola, Sanny S. W. Chung, et al. Mammalian E-type Cyclins Control Chromosome Pairing, Telomere Stability and CDK2 Localization in Male Meiosis. Plos Genetics. 2014;10(2):e1004165. https://doi.org/10.1371/journal. pgen.1004350.

Laiho, A., Kotaja, N., Gyenesei, A., & Sironen, A. Transcriptome profiling of the murine testis during the first wave of spermatogenesis. PLoS One. 2013;8(4): e61558. https://doi.org/10.1371/journal.pone.0061558.

Leitch, A.R. & Leitch, I.J. Genomic plasticity and the diversity of polyploid plants. Science. 2008;320(5875):481-483. https://doi.org/10.1126/science.1153585.

Manyes L, Holst S, Lozano M, Santos E, Fernandez-Medarde A. Spatial learning and long-term memory impairments in RasGrf1 KO, Pttg1 KO, and double KO mice. Brain Behav. 2018;8(11):e01089. https://doi.org/10.1002/brb3.1089.

Mark, M., Jacobs, H., Oulad-Abdelghani, M., Dennefeld, C., Feret, B., Vernet, N., Codreanu, C. A., Chambon, P., & Ghyselinck, N. B. STRA8-deficient spermatocytes initiate, but fail to complete, meiosis and undergo premature chromosome condensation. J Cell Sci. 2008;121(19):3233-3242. https://doi.org/10.1242/jcs.035071

Near, T. J. et al. Resolution of ray-finned fish phylogeny and timing of diversification. Proc. Natl Acad. Sci. USA. 2012;109(34):13698-13703 . https://doi.org/10.1073/pnas. 1206625109.

Nwachi O F, Esa Yuzine B. Comparative growth and survival of diploid and triploid Mozambique tilapia (*Oreochromism ossambicus*) reared in indoor tanks. Journal of environmental biology. 2016;37(4 Spec No):839-843.

Offenberg H H, Schalk J A, Meuwissen R L, van Aalderen M, KesterH A, Dietrich A J, Heyting C. SCP2: A major protein component of the axial elements of synaptonemal complexes of the rat. Nucleic AcidsResearch, 1998;26(11):2572-2579. https:// doi.org/10.1093/nar/26.11.2572.

Paneru B, Ali A, Al-Tobasei R, Kenney B, Salem M. Crosstalk among lncRNAs, microRNAs and mRNAs in the muscle 'degradome' of rainbow trout. Sci Rep. 2018 ;8(1):8416. https://doi.org/10.1038/s41598-018-26753-2.

Park In-Seok, Gil Hyun Woo, Lee Tae Ho, et al. Comparative Study of Growth and Gonad Maturation in Diploid and Triploid Marine Medaka, Oryzias dancena. Developmant & Reproduction. 2016;20(4):305-314. https://doi.org/10.12717/DR. 2016.20.4.305.

Pittman,D.L., Cobb,J., Schimenti,K.J., Wilson,L.A., Cooper,D.M., Brignull,E., Handel, M.A. and Schimenti,J.C. Meiotic prophase arrest with failure of chromosome synapsis in mice deficient for Dmc1, a germline-specific Rec A homolog. Molecular Cell. 1998;1(5), 697-705. https://doi.org/10.1016/S1097-2765(00)80069-6.

Punta, M., Coggill, P. C., Eberhardt, R. Y., Mistry, J., Tate, J., Boursnell, C., Pang, N., Forslund, K., Ceric, G., Clements, J., Heger, A., Holm, L., Sonnhammer, E. L., Eddy, S. R., Bateman, A., & Finn, R. D. The Pfam protein families database. Nucleic Acids Res. 2012;40(Database issue):D290-301. https://doi.org/10.1093/nar/gkr1065.

Reza AMMT, Choi YJ, Han SG, Song H, Park C, Hong K, Kim JH. Roles of microRNAs in mammalian reproduction: from the commitment of germ cells to peri-implantation embryos. Biol Rev Camb Philos Soc. 2019;94(2):415-438. https://doi.org/10.1111/brv.12459.

Sauer K, Lehner CF. The role of cyclin E in the regulation of entry into Sphase. Progress Cell Cycle Res. 1995;1:125-39. https://doi.org/10.1007/978-1-4615-1809 -9-10.

Schalk J A, Offenberg H H, Peters E, Groot N P, Hoovers J M, Heyting C. Isolation and characterization of the human SCP2 cDNA and chromosomal localization of the gene. Mammalian Genome,1999;10(6):642-644. https://doi.org/10.1007/s003359 901062.

Shu Y, Zhang H, Cai Q, Tang D, Wang G, Liu T, Lv B, Wu H. Integrated mRNA and miRNA expression profile analyses reveal the potential roles of sex-biased miRNA-mRNA pairs in gonad tissues of the Chinese concave-eared torrent frog (*Odorrana tormota*). J Exp Zool B Mol Dev Evol. 2019;332(3-4):69-80. https://doi.org/10.1002/jez.b.22851.

Stenberg, P., & Saura, A. Meiosis and its deviations in polyploid animals. Cytogenet Genome Res. 2013;140(2-4):185-203. https://doi.org/10.1159/000351731.

Sun, L., Luo, H., Bu, D., Zhao, G., Yu, K., Zhang, C., Liu, Y., Chen, R., & Zhao, Y. Utilizing sequence intrinsic composition to classify protein-coding and long non-coding transcripts. Nucleic Acids Res. 2013;41(17):e166. https://doi.org/ 10.1093/nar/gkt646.

Takemoto K, Imai Y, Saito K, et al. Sycp2 is essential for synaptonemal complex assembly, early meiotic recombination and homologous pairing in zebrafish spermatocytes. PLoS Genetics. 2020;16(2):e1008640. https://doi.org/10.1371/journal. pgen.1008640.

Taranger GL, et al. Risk assessment of the environmental impact of Norwegian Atlantic salmon farming. ICES J. Marine Sci. 2015;72:997-1021. https://doi.org/ 10.1093/ icesjms/fsu132.

Taylor, D. H., Chu, E. T., Spektor, R., & Soloway, P. D. Long non-coding RNA regulation of reproduction and development. Mol Reprod Dev. 2015;82(12):932-956. https://doi.org/10.1002/mrd.22581.

Teng Y, Wang Y, Fu J, Cheng X, Miao S, Wang L. Cyclin T2: a novel miR-15a target gene involved in early spermatogenesis. FEBS Lett. 2011;585(15):2493-500. https://doi.org/10.1016/j.febslet.2011.06.031.

Tiwary, B.K., Kirubagaran, R., Raym, A.K. The biology of triploid fish. Rev Fish Biol Fish. 2004;14:391-402. https://doi.org/10.1007/s11160-004-8361-8.

Van de Peer Y, et al. The evolutionary significance of ancient genome duplications. Nat Rev Genet. 2009;10:725-32. https://doi.org/10.1038/nrg2600.

Winkel K, Alsheimer M, Ollinger R, Benavente R. Protein SYCP2 provides a link between transverse filaments and lateral elements ofmammalian synaptonemal complexes. Chromosoma. 2009;118(2):259-267. https://doi.org/10.1007/s00412-008 -0194-0.

Xu, G., Huang, T., Jin, X., Cui, C., Li, D., Sun, C., Han, Y., & Mu, Z. Morphology, sex steroid level and gene expression analysis in gonadal sex reversal of triploid female (XXX) rainbow trout (*Oncorhynchus mykiss*). Fish Physiol Biochem. 2016;42(1):193-202. https://doi.org/10.1007/s10695-015-0129-7.

Yang F, Fuente R D L, Leu N A, et al. Mouse SYCP2 Is Required for Synaptonemal Complex Assembly and Chromosomal Synapsis during Male Meiosis. Journal of Cell Biology. 2006;173(4):497-507. https://doi.org/10.1083/jcb.200603063.

Yang, F., Guan, J., Li, R., Li, X., Niu, J., Shang, R., Qi, J., & Wang, X. miR-1388 regulates the expression of nectin2l in Paralichthys olivaceus. Comp Biochem Physiol Part D Genomics Proteomics. 2018;28:9-16. https://doi.org/10.1016/j.cbd. 2018.05.003.

Ye, W., Lv, Q., Wong, C. K., Hu, S., Fu, C., Hua, Z., Cai, G., Li, G., Yang, B. B., & Zhang, Y. The effect of central loops in miRNA:MRE duplexes on the efficiency of miRNA-mediated gene regulation. PLoS One. 2008;3(3):e1719. https://doi.org/ 10.1371/journal.pone.0001719.

Yin, C., Zhang, J., Shi, Z., Sun, W., Zhang, H., & Fu, Y. Identification and expression of the target gene emx2 of miR-26a and miR-26b in Paralichthys olivaceus. Gene. 2015;570(2): 205-212. https://doi.org/10.1016/j.gene.2015.06.030.

Yuan L, Liu JG, Zhao J, et al. The murine SCP3 gene is required for synaptonemal complex assembly, chromosome synapsis, and male fertility. Mol Cell. 2000;5:73-83.https://doi.org/10.1016/S1097-2765(00)80404-9.

Zhang, Y. C., Liao, J. Y., Li, Z. Y., Yu, Y., Zhang, J. P., Li, Q. F., Qu, L. H., Shu, W. S. & Chen, Y. Q. Genome-wide screening and functional analysis identify a large number of long noncoding RNAs involved in the sexual reproduction of rice. Genome Biol. 2014;15(12):512. https://doi.org/10.1186/s13059-014-0512-1.

Tables

Table 1. Overlapped DE miRNAs during gonadal development between the diploid and triploid rainbow trout.

MicroRNA	Sequence
ssa-miR-730a-5p	TCCTCATTGTGCATGCTGTGTG
dre-miR-26a-5p_R+2_1ss17TG	TTCAAGTAATCCAGGAGAGGCTTT
ola-miR-199a-3p_L+1R+1	AACAGTAGTCTGCACATTGGTTAT
PC-5p-21854_317	TGGATACAATTGAGTTTTGGAT
oni-miR-1388_1ss1AT	TGGACTGTCCAACCTGAGAATG
PC-5p-28329_238	CCCTGTTGTACTTCTCCTGC

Table 2. KEGG pathway enrichment of the overlapped DEGs

Pathway ID	Pathway Name	Genes	*p* value
ko04721	Synaptic vesicle cycle	SYT1, Snap25a, Rab3c	0.00
ko00330	Arginine and proline metabolism	Arg2, CNDP2, CKB	0.00
ko05162	Measles	mx2, mx	0.00
ko00514	Other types of O-glycan biosynthesis	B3gat1, Fut9	0.01
ko04911	Insulin secretion	Snap25a, Rab3c	0.01
ko05164	Influenza A	mx2, mx	0.02
ko04390	Hippo signaling pathway	Sox19b, Sox21b	0.02
ko03320	PPAR signaling pathway	MMP13, Hpx	0.04
ko00053	Ascorbate and aldarate metabolism	PITPNM2	0.04

Table 3. The DE mRNAs enriched in oocyte meiosis/homologous recombination pathway

Days post fertilization	DEmRNAs related to oocyte meiosis/homologous recombination
65 dpf	*sycp3*
180 dpf	*ccne1, calml4, cpeb2, adcy6, dmc1, kank1, kank4, ppp1cb, pvalb1*
600 dpf	*sycp2, sycp3, dmc1, adcy6, recql4, plk1, cpeb4, cdc25c, fbox5, ccnb1, ccne1, ccne2, aurkc, pttg1, mos*

Table 4. The predicted lncRNAs regulated indirectly *ccne1*

DE mRNA	Targeted DE miRNA	DE lncRNA	Strand	chromosome	Exons	Length (bp)
ccne1	dre-miR-15a-5p_R+1	MSTRG.74687.3	-	chrNW_018550071.1	2	1648
		MSTRG.76205.1	-	chrNW_018557577.1	1	1568
		MSTRG.30919.1	-	chr2	1	4938
		MSTRG.82739.1	+	chrNW_018592375.1	1	1985
		MSTRG.9268.1	-	chr12	1	8333
		MSTRG.63320.1	-	chr8	1	2693

Figures

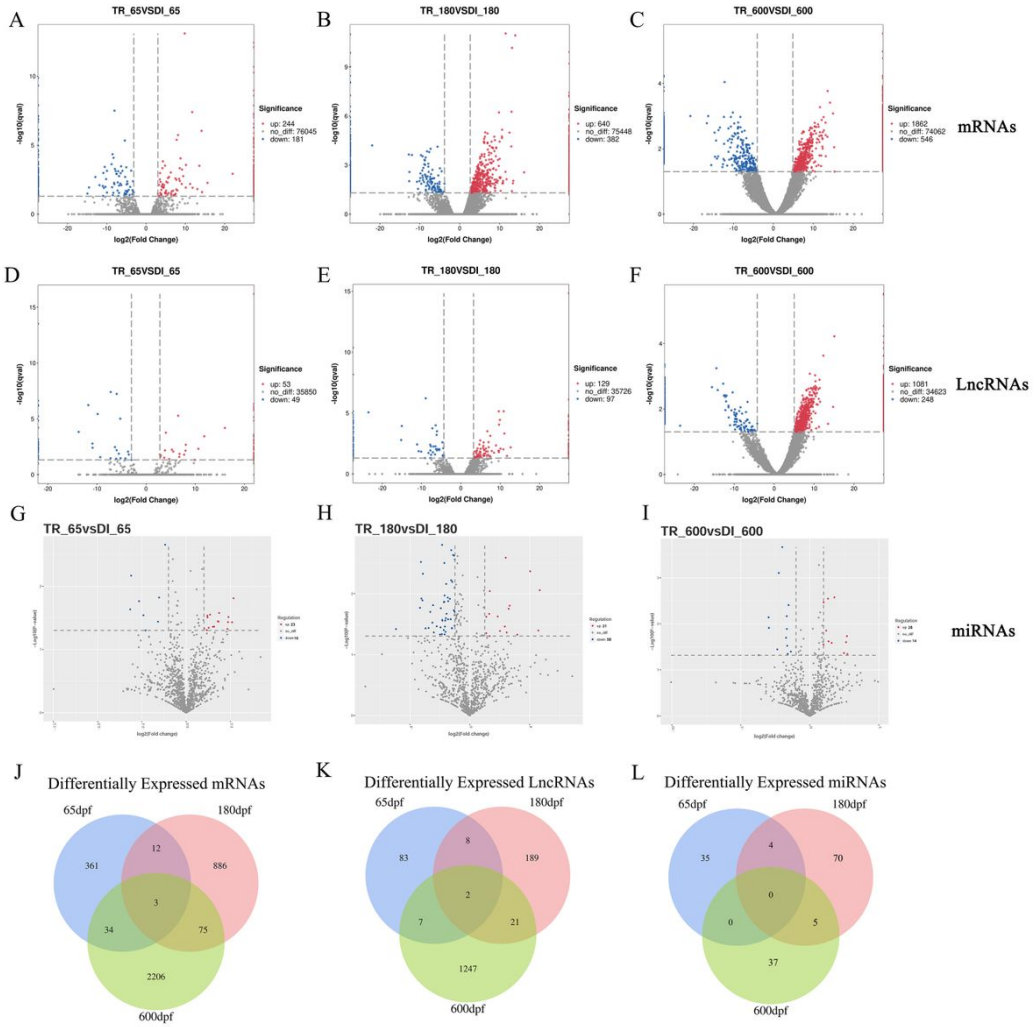

Figure 1

Identification of the overlapping DE mRNAs, DE lncRNAs, and DE miRNAs related to gonadal development. (A–C) Volcano plots of DE mRNAs in the triploid (XXX) and diploid (XX) gonads at 65 dpf, 180 dpf, and 600 dpf. (D–F) Volcano plots for DE lncRNAs in the triploid (XXX) and diploid (XX) gonads at 65 dpf, 180 dpf, and 600 dpf. (G–I) Volcano plots for DE miRNAs in the triploid (XXX) and diploid (XX) gonads at 65 dpf, 180 dpf, and 600 dpf. (J) Venn diagram for the overlapping DE mRNAs of 65 dpf, 180 dpf, and 600 dpf. (K) Venn diagram for the overlapping DE lncRNAs of 65 dpf, 180 dpf, and 600 dpf. (L) Venn diagram for the overlapping DE miRNAs of 65 dpf, 180 dpf, and 600 dpf.

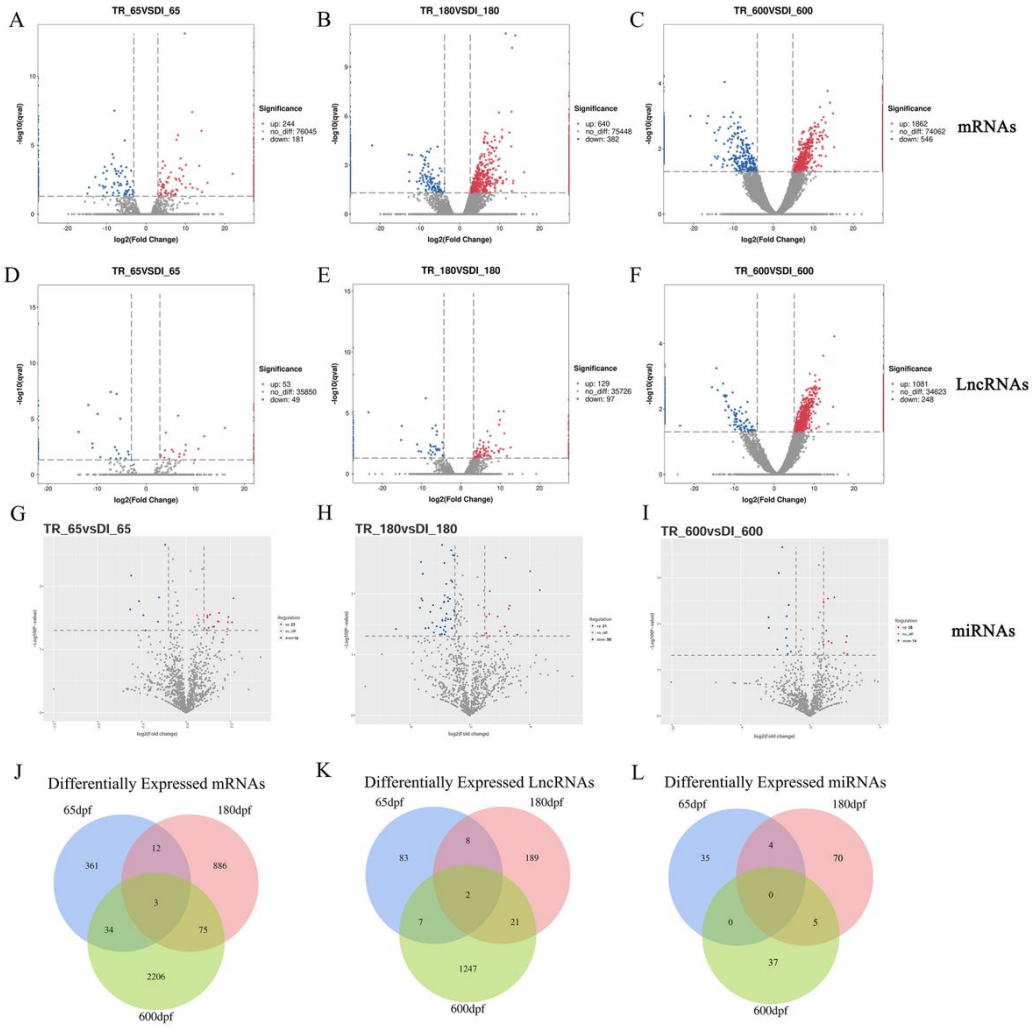

Figure 1

Identification of the overlapping DE mRNAs, DE lncRNAs, and DE miRNAs related to gonadal development. (A–C) Volcano plots of DE mRNAs in the triploid (XXX) and diploid (XX) gonads at 65 dpf, 180 dpf, and 600 dpf. (D–F) Volcano plots for DE lncRNAs in the triploid (XXX) and diploid (XX) gonads at 65 dpf, 180 dpf, and 600 dpf. (G–I) Volcano plots for DE miRNAs in the triploid (XXX) and diploid (XX) gonads at 65 dpf, 180 dpf, and 600 dpf. (J) Venn diagram for the overlapping DE mRNAs of 65 dpf, 180 dpf, and 600 dpf. (K) Venn diagram for the overlapping DE lncRNAs of 65 dpf, 180 dpf, and 600 dpf. (L) Venn diagram for the overlapping DE miRNAs of 65 dpf, 180 dpf, and 600 dpf.

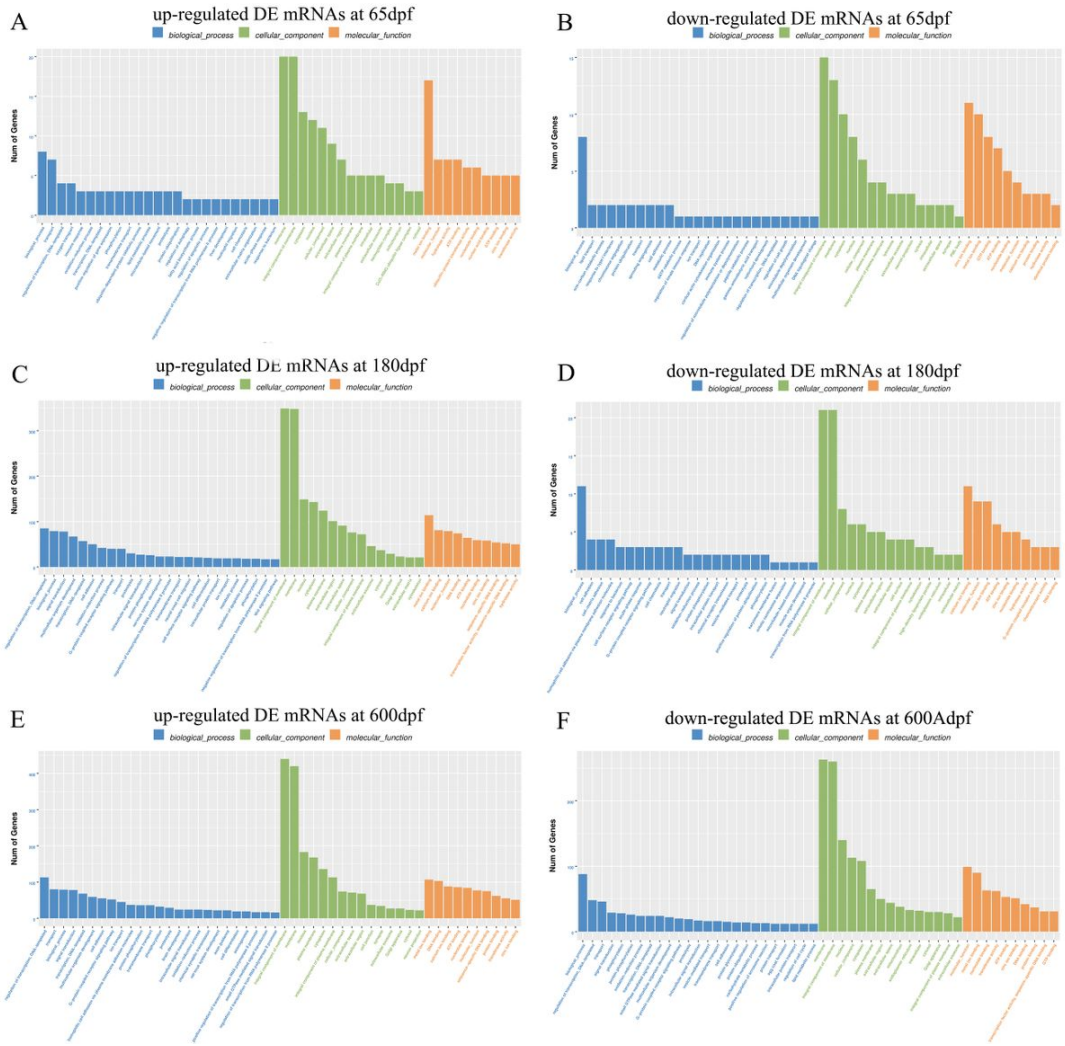

Figure 2

GO analysis of the differentially expressed mRNAs at each developmental point according to the up- and down- regulated DE mRNAs. (A) GO analysis of up-regulated DE mRNAs at 65 dpf. (B) GO analysis of down-regulated DE mRNAs at 65 dpf. (C) GO analysis of up-regulated DE mRNAs at 180 dpf. (D) GO analysis of down-regulated DE mRNAs at 180 dpf. (E) GO analysis of up-regulated DE mRNAs at 600 dpf. (F) GO analysis of down-regulated DE mRNAs at 600 dpf.

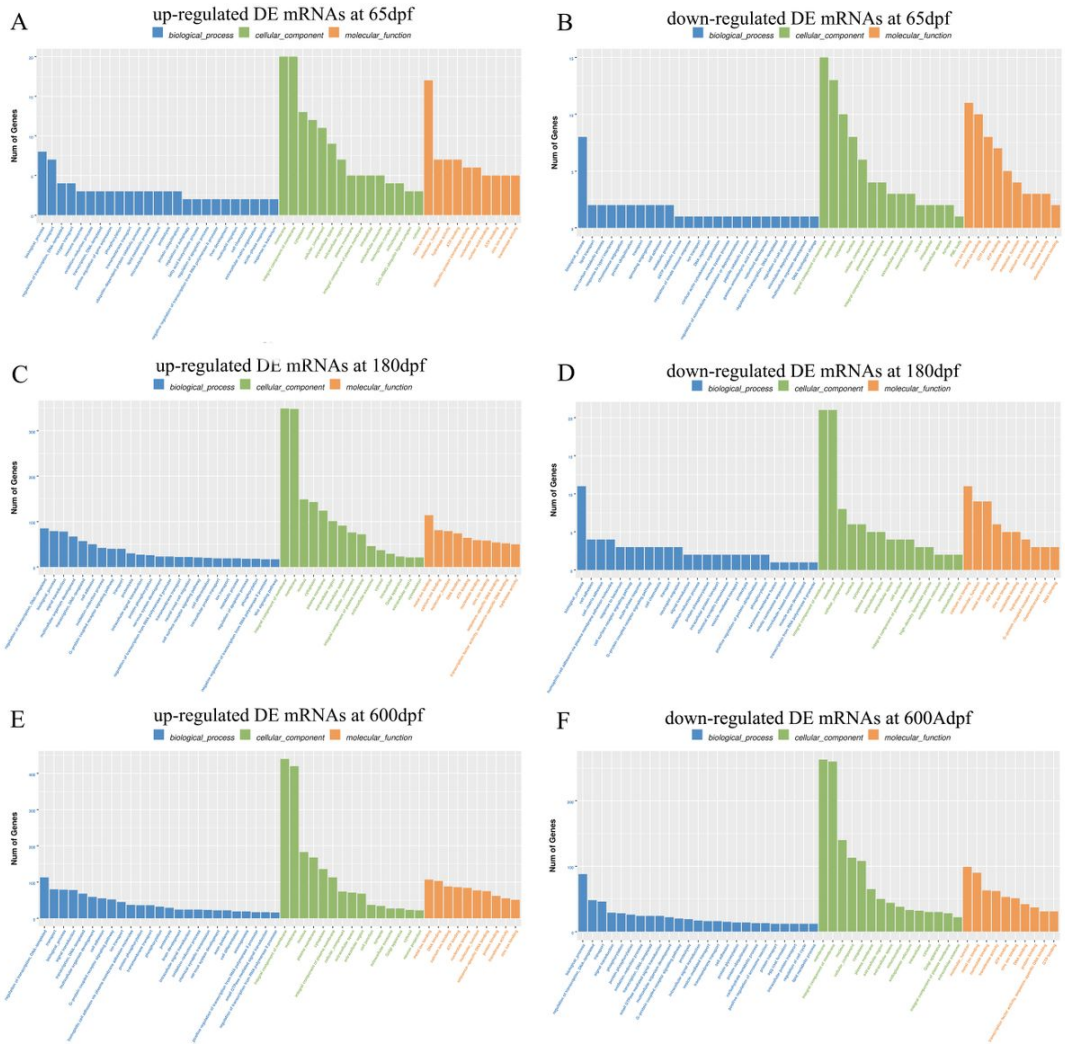

Figure 2

GO analysis of the differentially expressed mRNAs at each developmental point according to the up- and down- regulated DE mRNAs. (A) GO analysis of up-regulated DE mRNAs at 65 dpf. (B) GO analysis of down-regulated DE mRNAs at 65 dpf. (C) GO analysis of up-regulated DE mRNAs at 180 dpf. (D) GO analysis of down-regulated DE mRNAs at 180 dpf. (E) GO analysis of up-regulated DE mRNAs at 600 dpf. (F) GO analysis of down-regulated DE mRNAs at 600 dpf.

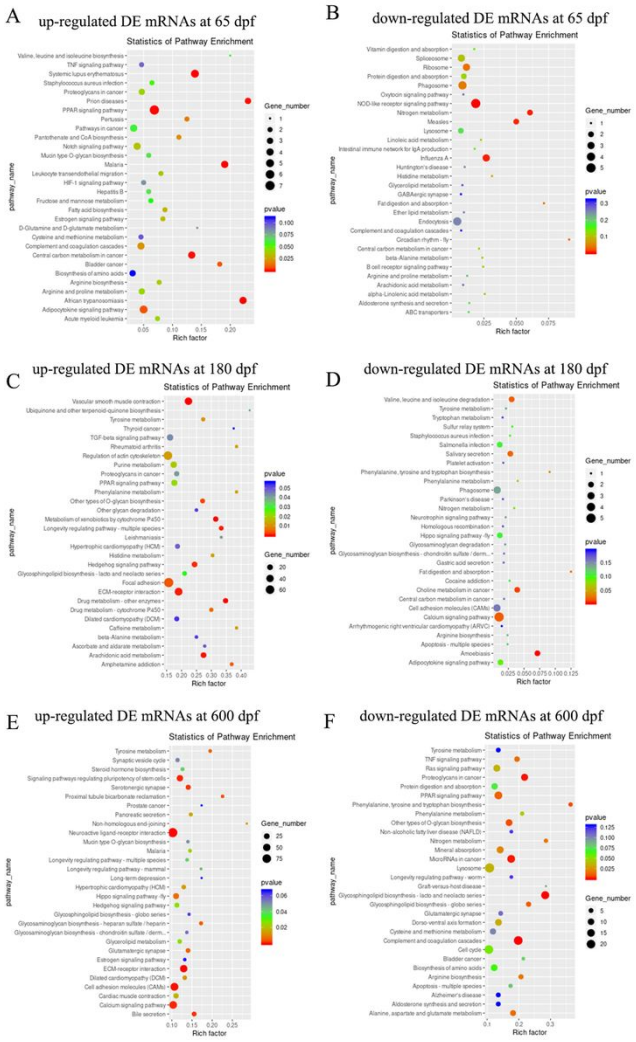

Figure 3

KEGG pathway analysis of the differentially expressed mRNAs at each developmental point according to the up- and down- regulated DE mRNAs. (A) KEGG analysis of up-regulated DE mRNAs at 65 dpf. (B) KEGG analysis of down-regulated DE mRNAs at 65 dpf. (C) KEGG analysis of up-regulated DE mRNAs at 180 dpf. (D) KEGG analysis of down-regulated DE mRNAs at 180 dpf. (E) KEGG analysis of up-regulated DE mRNAs at 600 dpf. (F) KEGG analysis of down-regulated DE mRNAs at 600 dpf.

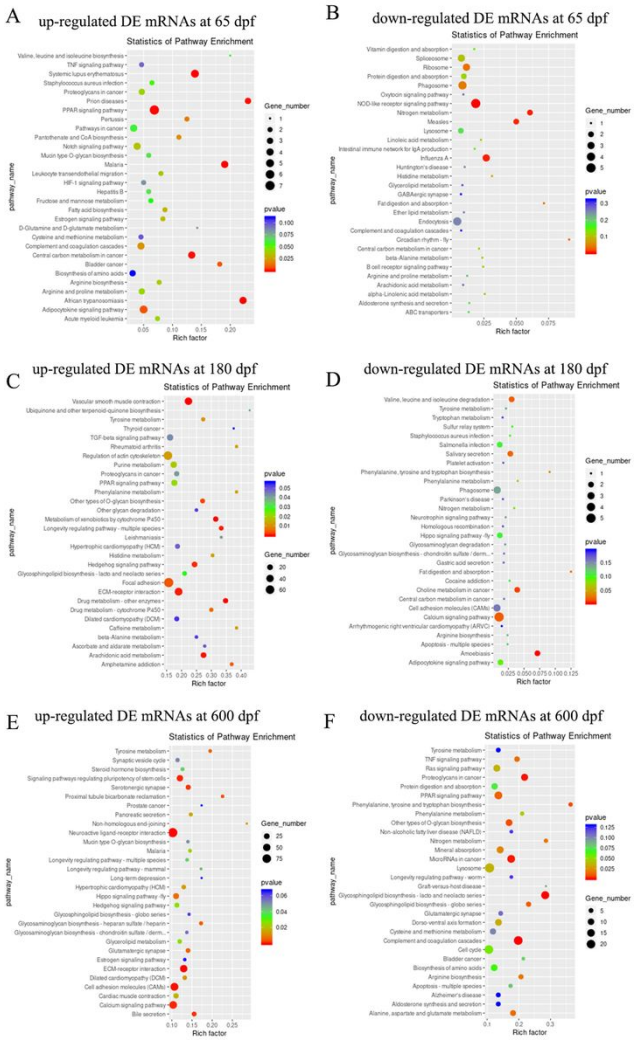

Figure 3

KEGG pathway analysis of the differentially expressed mRNAs at each developmental point according to the up- and down- regulated DE mRNAs. (A) KEGG analysis of up-regulated DE mRNAs at 65 dpf. (B) KEGG analysis of down-regulated DE mRNAs at 65 dpf. (C) KEGG analysis of up-regulated DE mRNAs at 180 dpf. (D) KEGG analysis of down-regulated DE mRNAs at 180 dpf. (E) KEGG analysis of up-regulated DE mRNAs at 600 dpf. (F) KEGG analysis of down-regulated DE mRNAs at 600 dpf.

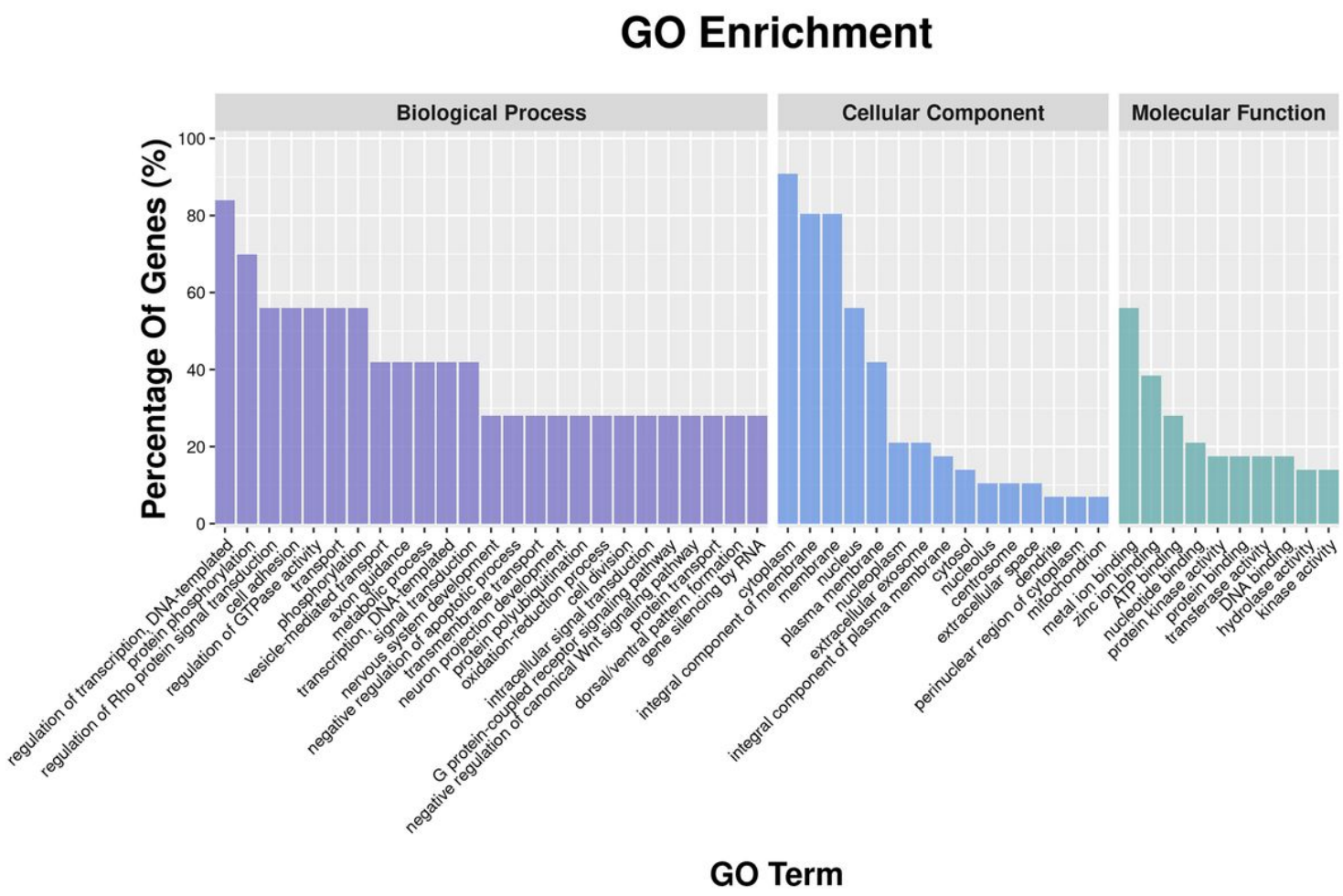

Figure 4

GO analysis of the overlapping DE mRNAs of 65 dpf, 180 dpf, and 600 dpf.

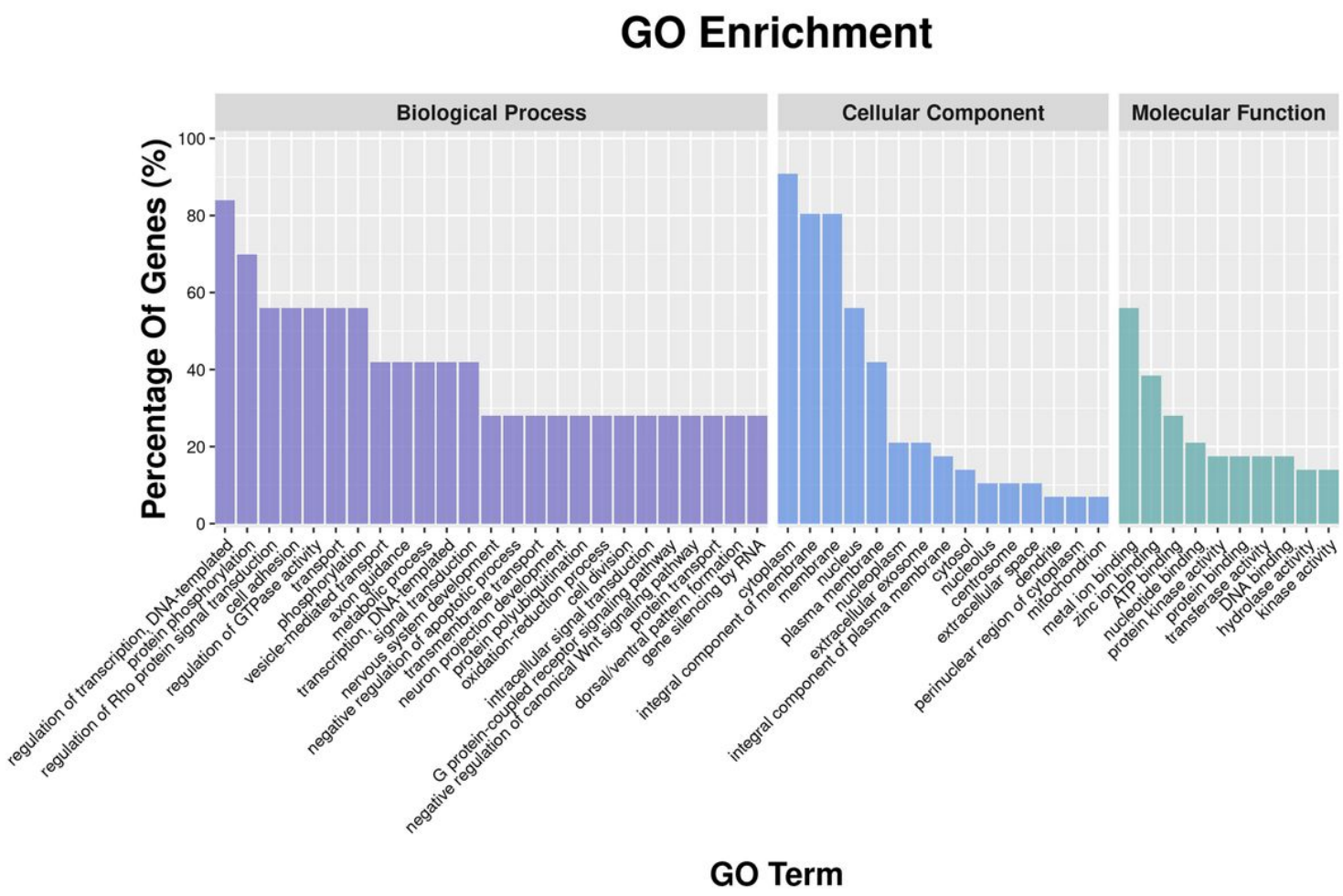

Figure 4

GO analysis of the overlapping DE mRNAs of 65 dpf, 180 dpf, and 600 dpf.

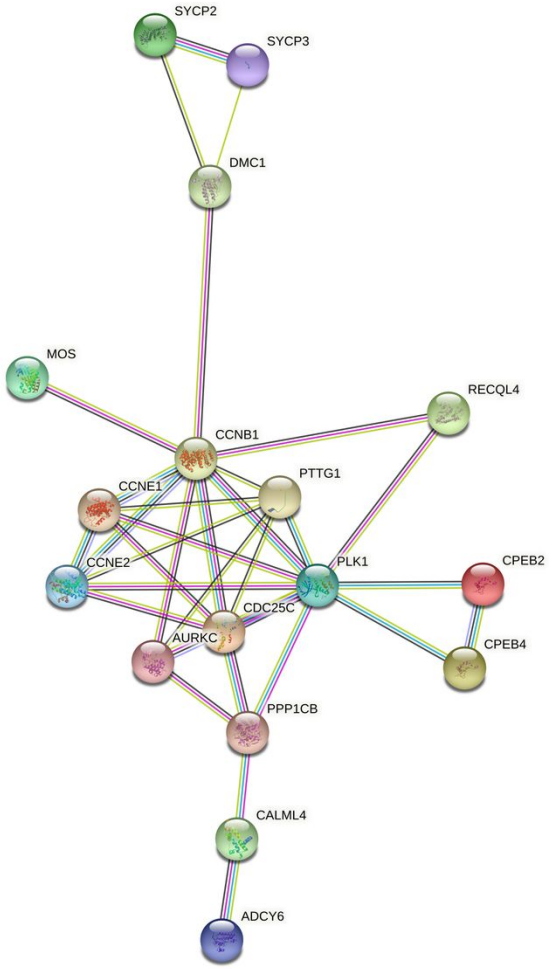

Figure 5

The protein-protein interaction (PPI) network of DE mRNAs related to oocyte meiosis and homologous recombination.

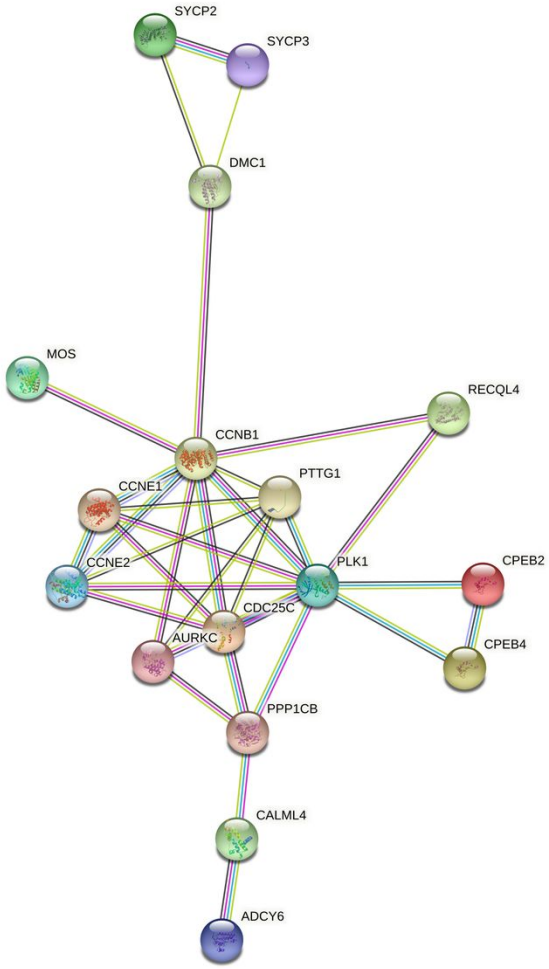

Figure 5

The protein-protein interaction (PPI) network of DE mRNAs related to oocyte meiosis and homologous recombination.

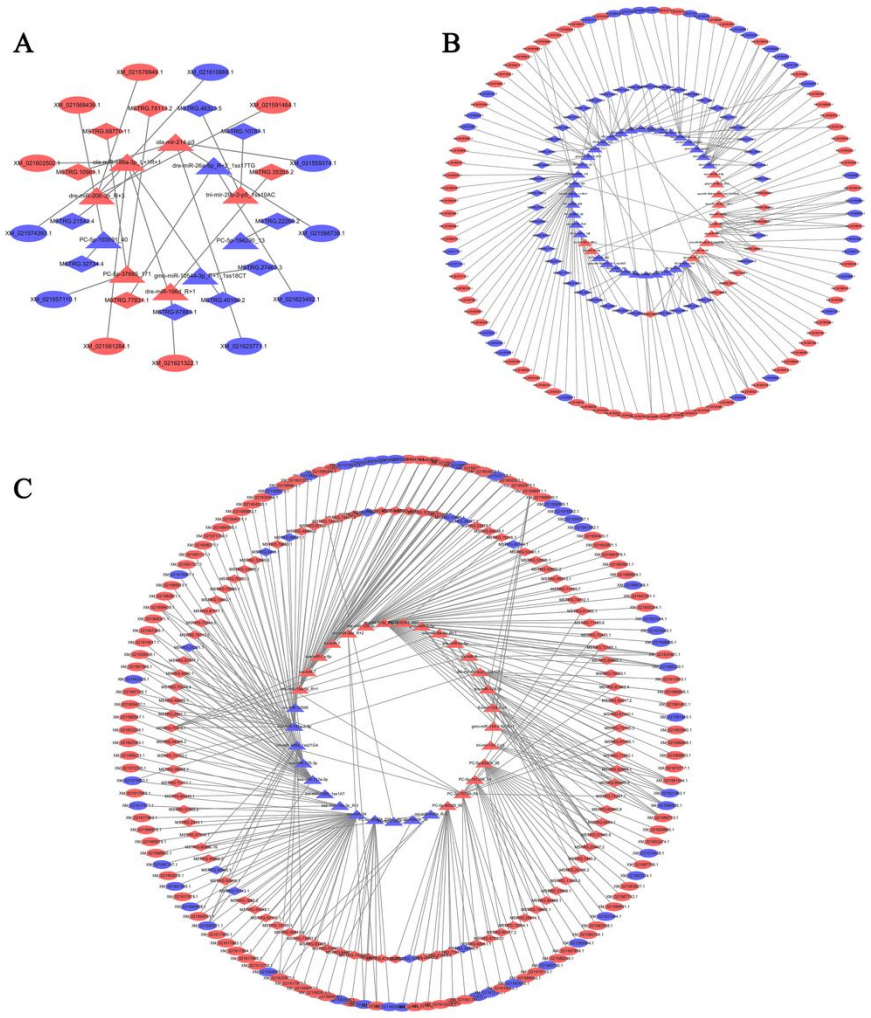

Figure 6

The predicted miRNA-mRNA/lncRNA interaction network of 65 dpf (A), 180 dpf (B) and 600 dpf (C). The ellipse represents mRNAs, the rectangle represents lncRNAs, and the triangle represents miRNAs. The colour of pink represents up-regulated nodes, and the colour of blue represents down-regulated nodes.

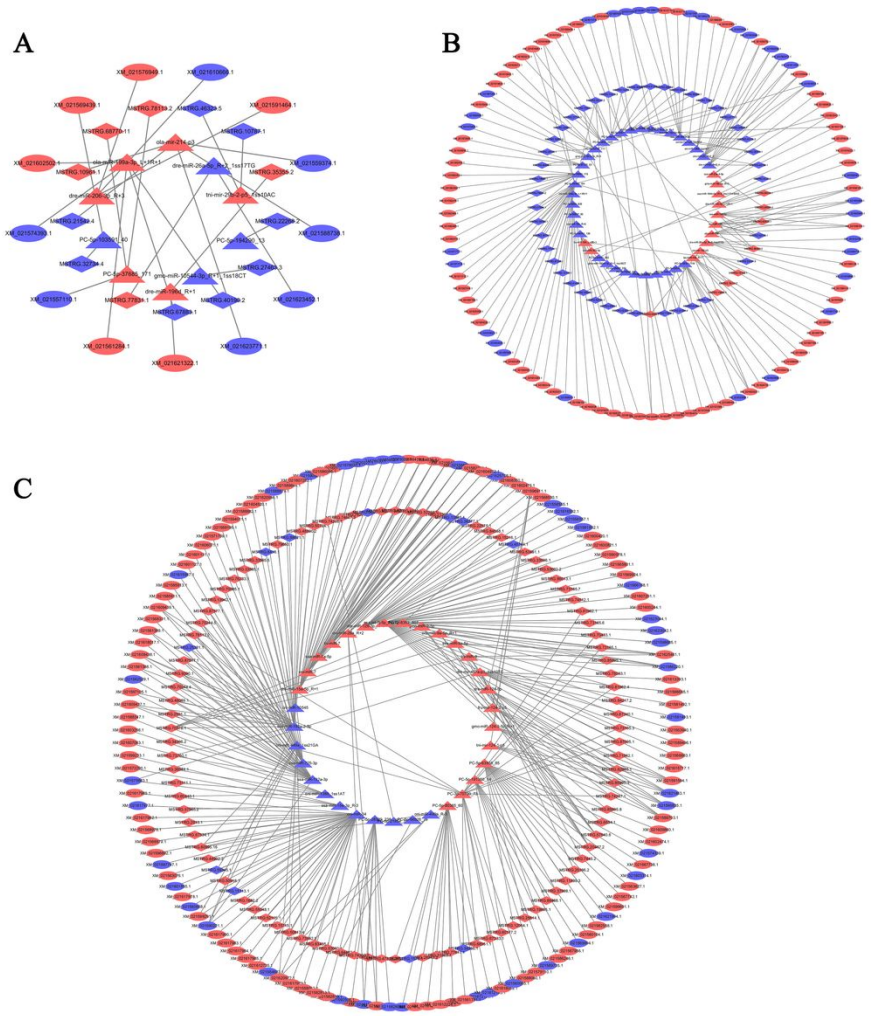

Figure 6

The predicted miRNA-mRNA/lncRNA interaction network of 65 dpf (A), 180 dpf (B) and 600 dpf (C). The ellipse represents mRNAs, the rectangle represents lncRNAs, and the triangle represents miRNAs. The colour of pink represents up-regulated nodes, and the colour of blue represents down-regulated nodes.

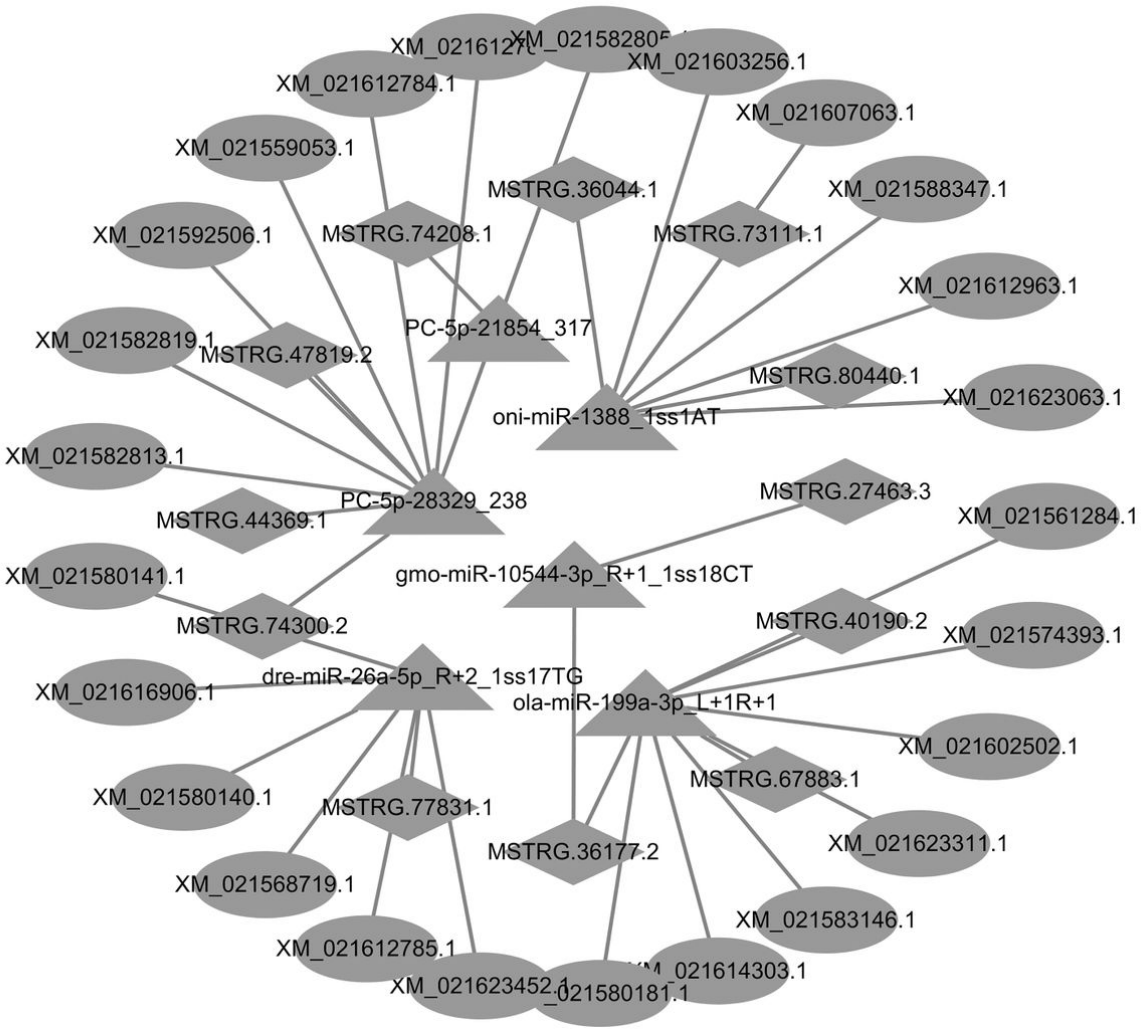

Figure 7

The predicted miRNA-mRNA/lncRNA interaction network based on overlapped DE RNAs from the three previously built networks for each timepoint in Figure 5. The network consisted of 6 DE miRNAs, 12 DE lncRNAs, and 25 DE mRNAs. The ellipse represents mRNAs, the rectangle represents lncRNAs, and the triangle represents miRNAs.

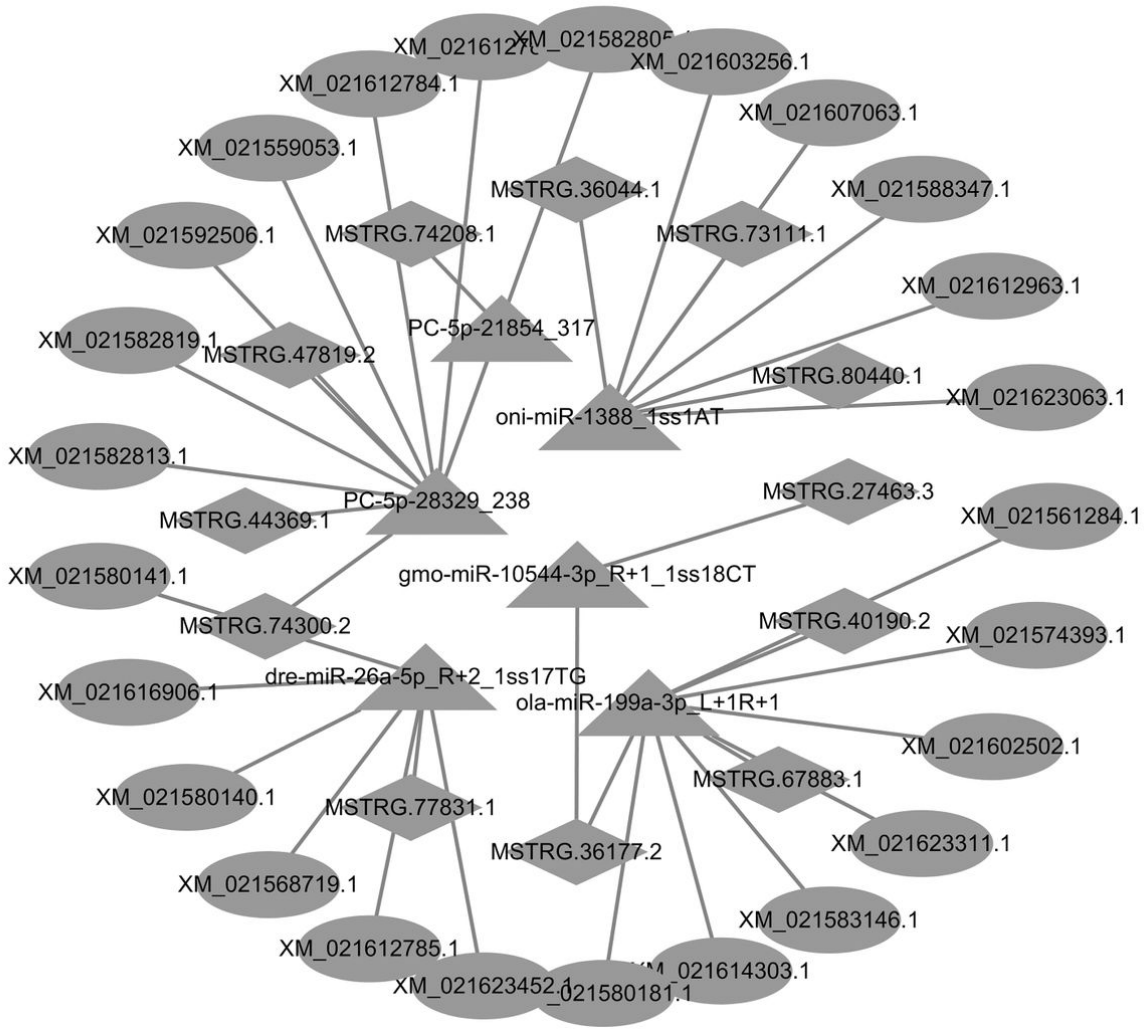

Figure 7

The predicted miRNA-mRNA/lncRNA interaction network based on overlapped DE RNAs from the three previously built networks for each timepoint in Figure 5. The network consisted of 6 DE miRNAs, 12 DE lncRNAs, and 25 DE mRNAs. The ellipse represents mRNAs, the rectangle represents lncRNAs, and the triangle represents miRNAs.

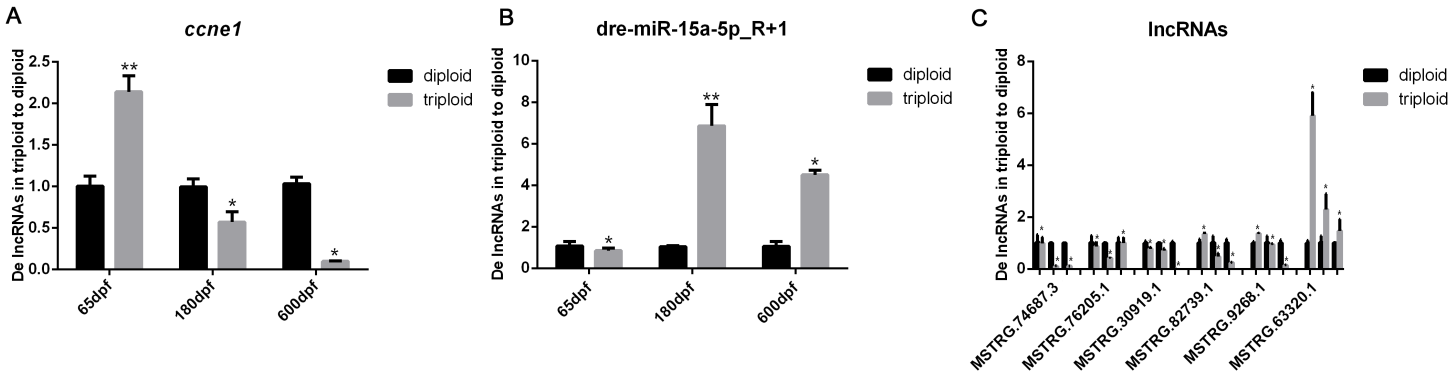

Figure 8

Validation of RNA expression by quantitative real-time PCR. (A) The expression of 7 ccne1 in gonad of triploid (XXX) rainbow trout as compared to that of the diploid (XX) at 65 dpf, 180 dpf, and 600 dpf. (B) The expression of dre-miR-15a-5p_R+1 in gonad of triploid rainbow trout as compared to that of the diploid at 65 dpf, 180 dpf, and 600 dpf. (C) The expression of 6 targeted lnRNAs in the gonad of triploid (XXX) rainbow trout as compared to that of the diploid (XX) at 65 dpf, 180 dpf, and 600 dpf. The values are represented as the means±SEM for three individuals. The significance was expressed "*" as a P-value of <0.05, and "**" as a P-value of < 0.01.

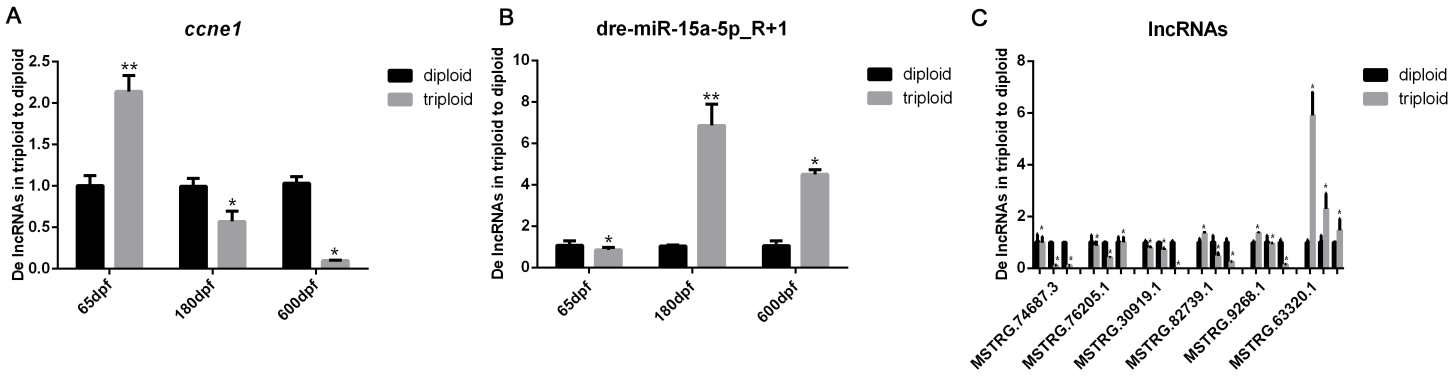

Figure 8

Validation of RNA expression by quantitative real-time PCR. (A) The expression of 7 ccne1 in gonad of triploid (XXX) rainbow trout as compared to that of the diploid (XX) at 65 dpf, 180 dpf, and 600 dpf. (B) The expression of dre-miR-15a-5p_R+1 in gonad of triploid rainbow trout as compared to that of the diploid at 65 dpf, 180 dpf, and 600 dpf. (C) The expression of 6 targeted lnRNAs in the gonad of triploid (XXX) rainbow trout as compared to that of the diploid (XX) at 65 dpf, 180 dpf, and 600 dpf. The values are represented as the means±SEM for three individuals. The significance was expressed "*" as a P-value of <0.05, and "**" as a P-value of < 0.01.

Supplementary Files

This is a list of supplementary files associated with this preprint. Click to download.

- FigureS1.jpg
- FigureS1.jpg
- FigureS2.jpg
- FigureS2.jpg
- FigureS3.jpg
- FigureS3.jpg
- TableS1.XLSX
- TableS1.XLSX
- TableS2.XLSX
- TableS2.XLSX
- TableS3.XLSX
- TableS3.XLSX
- TableS4.XLSX
- TableS4.XLSX
- TableS5.XLSX
- TableS5.XLSX
- TableS6.XLSX
- TableS6.XLSX
- TableS7.xlsx
- TableS7.xlsx
- TableS8.xlsx
- TableS8.xlsx
- TableS9.xlsx
- TableS9.xlsx
- TableS10.docx
- TableS10.docx
- TableS11.docx
- TableS11.docx
- TableS12.XLSX

- TableS12.XLSX
- TableS13.XLSX
- TableS13.XLSX
- TableS14.docx
- TableS14.docx